Precambrian Research 379 (2022) 106790

Contents lists available at ScienceDirect

Precambrian Research

journal homepage: www.elsevier.com/locate/precamres

Recording the largest gabbro-anorthositic complex worldwide: The Kunene Complex (KC), SW Angola

Carmen Rey-Moral [a,*], Tania Mochales [a], Enrique Merino Martínez [b], Jose Luis García Lobón [a], María Teresa López Bahut [a], Raquel Martín-Banda [a], María Carmen Feria [b], Dianne Ballesteros [c], Ana Machadinho [d,e], Daniela Alves [d]

[a] CN IGME-CSIC (Instituto Geológico y Minero de España-Consejo Superior de Investigaciones Científicas), c/ La Calera s/n, 28760 Tres Cantos, Madrid, Spain
[b] UTE PLANAGEO-IGME, c/ La Calera s/n, 28760 Tres Cantos, Madrid, Spain
[c] USB (Universidad Simón Bolívar), Valle de Sartenejas, Municipio Baruta, 1080 Caracas, Venezuela
[d] UTE PLANAGEO-LNEG, Estrada da Portela. Bairro do Zambujal, Apartado 7586-Alfragide. 2610-999 Amadora, Portugal
[e] CGEO - Geociences Center, University of Coimbra, Rua Sílvio Lima, Pólo II, 3030-790 Coimbra, Portugal

ARTICLE INFO

Keywords:
Gravity modelling
Angola
Kunene Complex (KC)
2.5D modelling

ABSTRACT

The Kunene Complex (KC) represents a large Mesoproterozoic igneous body, mainly composed of anorthosites and gabbroic rocks that extends from SW Angola to NW Namibia (18000 km^2, N-S trend, and ca. 350 km long and 25–50 km wide). Although the KC has been studied from a cartographic and geochemical point of view, little is known about its structure at depth below the sedimentary deposits of the Kalahari basin. Hence, we use available satellite gravity data to estimate its extent and to unravel its morphology at depth. The Bouguer anomaly map depicts a gravity gradient from the coast (+200 mGal) towards eastern Angola (-150 mGal), which is explained by the transition from a young, dense and thin basaltic oceanic crust, formed during the Mesozoic Atlantic rifting, to an old, light and thick Archaean to Proterozoic continental crust (Congo Craton), to the east. The outcropping KC interrupts the gravity trend, showing at the western, southwestern and northeastern sides, several positive and isolated gravity anomalies linked to gabbroic intrusions associated to KC (ca. 50 km wavelength and −90 mGal). In contrast, the anomalies found at the central part of the massif (50 km wavelength and < -110 mGal) correspond to the dominant anorthositic members, according to the spatial correlation of the mapping. Five 2.5D gravity profiles have been modelled to investigate the unexposed eastern boundary, reconstructing the surface crustal structure (between 0 and 15 km depth) overlaid by the thin sedimentary cover of the Kalahari basin. The gravity modelling helps us to show that the KC was emplaced in the Upper Crust and extends in depth up to ca. 6 km, showing a lobular geometry and following a large NE-SW to NNE-SSW linear trend, presumably inherited from older Palaeoproterozoic structures. The lateral continuation of the KC to the east (between 50 and 125 km) beneath the Kalahari sediments suggests an overall size of at least twice the outcropping dimension (about 42500 km^2). This statement clearly influences in the economic potential of this massif, related to the prospecting of raw materials and certain types of economic mineralization (Fe-Ti oxides, metallic sulphides or platinum group minerals).

1. Introduction

The Kunene Complex (KC) is one of the largest exposed Proterozoic massif-type anorthosite intrusions of the world (e.g., Ashwal and Twist, 1994; Drüppel et al., 2007). It was emplaced during Mesoproterozoic times (Kibaran Event; Tack et al., 2010) in the southwestern part of the Congo Craton – the Angolan Shield – cropping out in the SW and NW parts of Angola and Namibia, respectively (Fig. 1). The Congo Craton is one of the approximately 35 fragments remaining of the last Archaean/Paleoproterozoic supercontinent (Bleeker, 2003). The Archaean cores of the Congo (-São Francisco) Craton were accreted to other major Archaean to Palaeoproterozoic terrains (i.e., Amazonia, West Africa,

* Corresponding author.
E-mail addresses: c.rey@igme.es (C. Rey-Moral), t.mochales@igme.es (T. Mochales), enrique.merino@uteplanageo.com (E. Merino Martínez), jl.garcia@igme.es (J.L. García Lobón), mt.lopez@igme.es (M.T. López Bahut), r.martin@igme.es (R. Martín-Banda), maria.feria@uteplanageo.com (M.C. Feria), ballesterosrda@gmail.com (D. Ballesteros), ana.machadinho@gmail.com, ana.machadinho@dct.uc.pt (A. Machadinho), danielapva@gmail.com (D. Alves).

https://doi.org/10.1016/j.precamres.2022.106790
Received 4 November 2021; Received in revised form 22 June 2022; Accepted 7 July 2022
Available online 28 July 2022

Kalahari and Río de la Plata) and smaller crustal blocks during Paleo-, Meso- and Neoproterozoic times through the Eburnean, Kibaran and Pan-African Belts (see Fig. 1), respectively (p.e. De Waele et al., 2008; Rapalini, 2013).

In Angola, the Eburnean and Pan-African Belts are well represented whereas the Kibaran Belt is not widely exposed (see Fig. 1). In the Angolan Shield, the Mesoproterozoic Kunene Complex (KC) is usually interpreted as the intraplate magmatic record of the Columbia/Nuna continental breakup (e.g., Meert 2012; Evans, 2013). The Kunene Complex intruded at the southern margin of the Congo Craton (i.e., the Angolan Shield), in the neighbourhood of the Pan-African Kaoko belt in southwestern Africa (Ashwal and Twist, 1994). It extends for about 18000 km^2 from southwestern Angola to northwestern Namibia, elongated in a N-S direction into the widespread Archaean to Paleoproterozoic reworked basement (Carvalho and de Alves, 1990). To the east, the Kunene Complex is mostly covered by the Kalahari sediments, which make it difficult to evaluate its actual extent (Morais et al., 1998). The Kunene complex is mainly composed of anorthosites and other anorthosite-like lithologies, mainly consisting of rocks bearing 80–90 vol% plagioclase with variable amounts of interstitial olivine and ortho/clinopyroxene (leucotroctolites, leuconorites and leucogabbros), that intruded mainly between 1438 and 1375 Ma (Baxe, 2007; Drüppel et al., 2007; Brower, 2017; Bybee et al., 2019). The oldest crystallization ages for the KC anorthosites and related rocks reported by Bybee et al. (2019), of 1503 Ma, probably reflect the earliest stages of this magmatism. Subordinate gabbros, norites and scarce ultramafic rocks, presumably related to the KC, are restricted to the border zone (Carvalho and de Alves, 1990; Silva, 1992; Ashwal and Twist, 1994; Drüppel et al., 2007; Maier et al., 2013). Minor coeval granite bodies ("Red Granites", syenites, mangerite dykes and related rocks) crop out dispersedly within

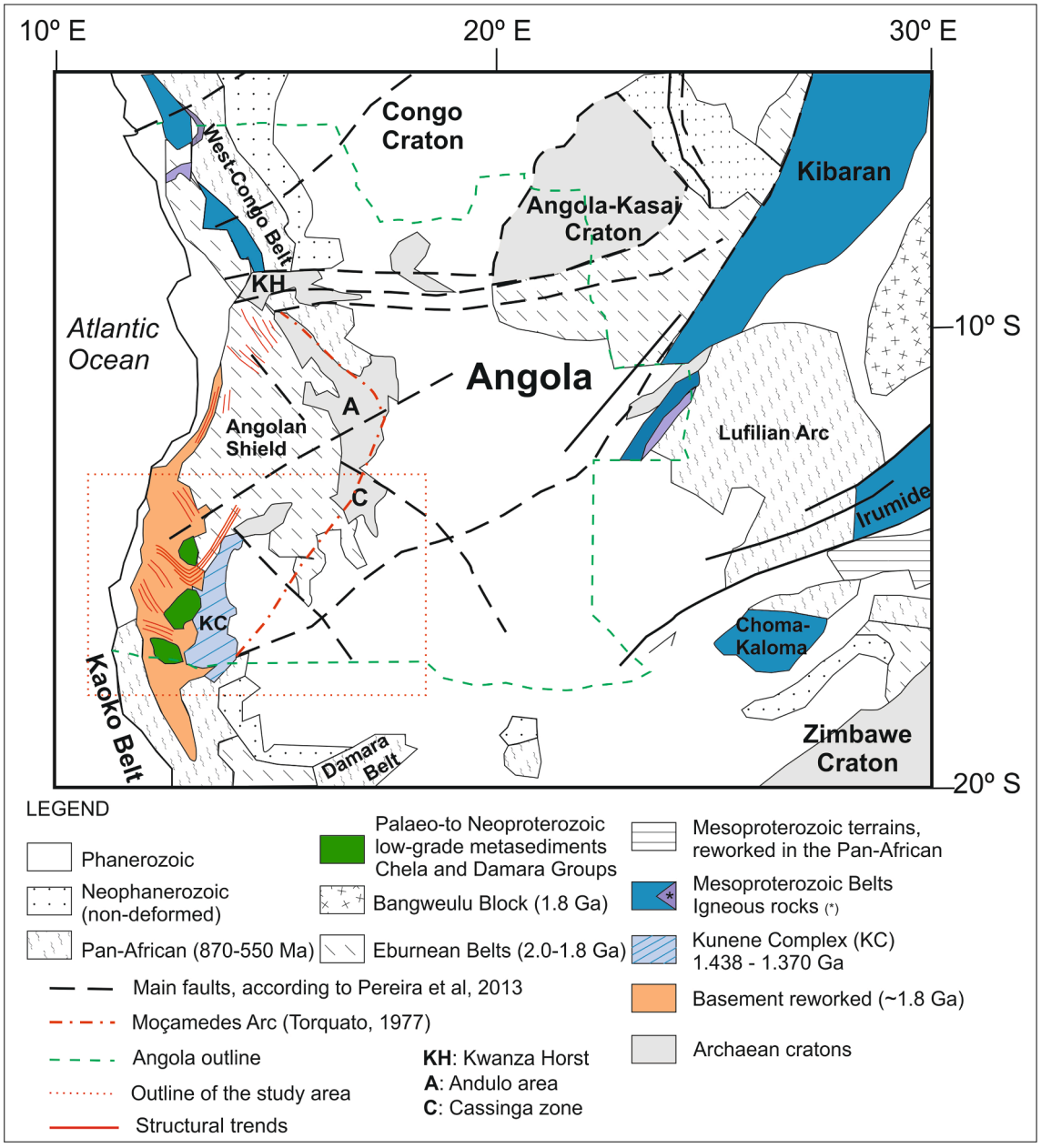

Fig. 1. Geological setting of the study area with the main geological units (modified from Hanson, 2003; Kröner and Cordani, 2003 and Pereira et al., 2013a, 2013b). The area of this work is squared in red dotted . Surrounding cratons and the Angolan shield are differentiated. Eburnean, Mesoproterozoic and Pan-African Belts are put in relation to the Kibaran Kunene Complex (KC), as well as to the reworked Basement and Mesoproterozoic reworked terrains. Some main lineation and arches are highlighted pertaining to the Kunene intrusive Complex.

the anorthosite massif and at the western and eastern margins of the KC. This regional magmatism has been interpreted as: (i) linked to one of the distinct Mesoproterozoic extensional intraplate events (between 1.5 and 1.1 Ga) associated to Large Igneous Provinces (LIPs), that intruded in a short time span linked to the Kibaran extension, showing U-Pb zircon ages mainly constrained between 1380 and 1370 Ma (Mayer et al., 2004; Tack et al. 2010; Ernst et al., 2013). Some authors (e.g. Mayer et al., 2004) argue for a thermal extensional event that promoted the separation of the Congo and Kaapvaal-Zimbabwe Cratons during the Mesoproterozoic; (ii) related to the crustal thickening episode occurred during Mesoproterozoic, in an E-W contractional regime, related to the Kibaran Belt (Brower, 2017; Bybee et al., 2019; Lehmann et al., 2020). Structural, petrological, geochemical and geochronological data suggest that this belt was formed following collision of the Congo Craton and the Tanzanian-Bangweulu cratonic block, and that such collision was preceded by subduction (Kampunzu et al., 1986; Kokonyangi, et al., 2005).

During the last decades, many investigations examined the petrogenesis of the Kunene Complex using whole-rock and isotope

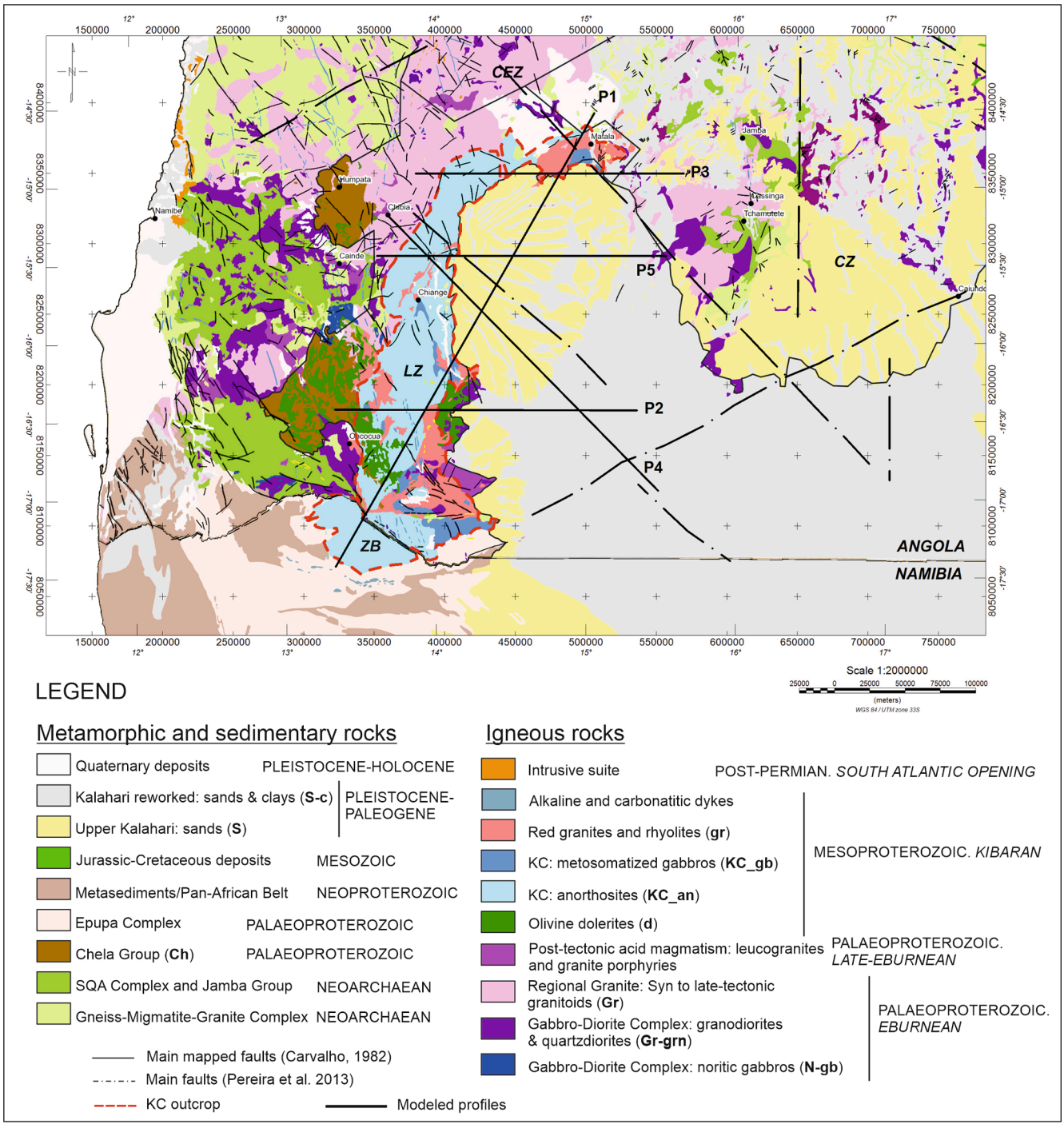

Fig. 2. Geological map of Angola (modified from Carvalho, 1982 and adapted by Pereira et al, 2013a, 2013b) and Namibia (synthetized from Kröner et al., 2010, 2015) with the main geological units (in parenthesis the acronym displayed in the 2.5D models). See the location of the five modelled profiles (P1, P2, P3, P4 and P5). The main faults, mapped by Carvalho, 1982 are shown in black thin lines. Pereira et al, 2013a, 2013b interpreted some NW-SE, NE-SW and N-S, main faults represented in black dashed-dotted lines. The outcrop of the KC is outlined in red dashed line. LZ: Lubango Zone; CZ: Casinga Zone and CEZ: Central Eburnean Zone (following McCourt et al. 2013). ZB: Zebra Mountains.

geochemical and geochronological methods, but no gravity modelling has been performed. Some previous works dealing with gravity and magnetic data can be found in Blanchar et al. (2017), that reports a magnetic and gravimetric study in the Kibarian Belt; Braitenberg (2015), compiling the Earth gravity data from satellite missions; and Finn et al. (2015), mapping the 3D extent of a mafic intrusion in South Africa. The aim of this paper is to decipher the deep geometry of the KC and the crystalline basement of SW Angola in a remote area where the unique public/open access gravity information, covering the whole study area, exists throughout the published data of the Bureau Gravimetrique International (Bonvalot et al., 2012). The Bouguer anomaly data is computed from the EGM2008 and the satellite data are the dominant source of information providing a uniform coverage. This gravimetric dataset is here used to define the unidentified geometry and extension of the plutonic complex under the Kalahari sediments, by means of 2.5D modelling and Euler deconvolution depths, providing new information on the KC.

2. Geological setting

The studied area is located at the southwesternmost part of Angolan shield, between the Eburnean Belt to the north and west, the Pan-African Kaoko Belt to the southwest and the Post-Permian sedimentary deposits of the Kalahari Group to the east (Figs. 1, 2; e.g., Carvalho, 1982; Pereira et al., 2013b). This area records a complex geological history comprising: i) the generation of an Archaean crust (De Waele et al., 2008); ii) the amalgamation of these cratonic pieces during the Palaeoproterozoic, related to the formation of the Columbia/Nuna Supercontinent during the Eburnean Orogeny (2.0–1.8 Ga; Delor et al., 2006; Pereira et al., 2013b); iii) the tectono-magmatic Mesoproterozoic event (Kibaran Event; Tack et al., 2010; Lehmann et al., 2020), associated with the breakup of Columbia and prior the amalgamation of Rodinia (Ernst et al., 2013); iv) the formation of the Gondwana Supercontinent during Neoproterozoic to early Palaeozoic times (Pan-African Event; e.g., De Wit and Linol; 2015); and v) the Pangea rupture and formation of the Atlantic Ocean in Mesozoic times (e.g., Marzoli et al., 1999; Marsh and Swart, 2018). The Archaean to Palaeoproterozoic basement is mainly composed of metasedimentary and igneous derived materials that were intensely deformed and metamorphosed during the Palaeoproterozoic, mostly related to the Eburnean orogeny. Large-scale calc-alkaline plutonic masses and scarce metasedimentary sequences of Palaeoproterozoic age are dominant in the area (Carvalho, 1982; Kröner et al., 2010, 2015; McCourt et al., 2013; Pereira et al., 2013a, 2013b; Jelsma et al., 2018). This crystalline basement was intruded during the Mesoproterozoic by a set of mafic dykes of 1.50 and 1.10 Ga (Ernst et al., 2013; Salminen et al., 2018), and by the large Kunene Complex (1438–1375 Ma; e.g., Mayer et al., 2004; Drüppel et al., 2007; Baxe, 2007; Bybee et al., 2019).

In SW and central Angola, the Eburnean basement forms an arched macrostructure, called as the Moçamedes Arc (Fig. 1; Torquato, 1977). The structure of the basement (Basement reworked in Fig. 1) follows a NW-SE to WNW-ESE-trend (see the structural trends within the Basement reworked) from the western edge of the Kunene Complex up to the southwestern end of Angola, where the structure is deflected by the Neoproterozoic NNW-SSE Kaoko Belt (Fig. 1). This NW-SE trend is apparently truncated by the intrusion of the Mesoproterozoic Kunene Complex (Fig. 1). On the other hand, the Archaean to Palaeoproterozoic basement found from the northwestern part of the KC towards the Andulo area is structured in an NNE-SSW direction, following an orientation nearly parallel to the Moçamedes Arc (Fig. 1). Finally, close to the Andulo region, the structures of the basement migrate back to a dominant NW-SE-trend, that continue towards the Kwanza Horst (Torquato, 1977; Jelsma et al., 2018; Fig. 1).

The most recent structures are interpreted as extensional fractures, mainly oriented in NNE-SSW direction together with ENE-WSW and WNW-ESE conjugated transcurrent fractures, probably related to the opening of the Atlantic Ocean in Mesozoic times (e.g., Torquato, 1977; Pereira et al., 2003). The geological record, regarding the distinct tectono-thermal events found at SW Angola, is described in the next sections.

2.1. The Archaean to Palaeoproterozoic metamorphic crust

The Archaean to Palaeoproterozoic basement of south-western Angola is composed of highly deformed orthogneisses and metasedimentary sequences, remobilized during the different Proterozoic tectono-thermal events (e.g., Jelsma et al., 2018). This medium- to high-grade metamorphic crust consists of the Jamba Group, the Gneissic-Migmatitic and Granitic Complex, and the Schist-Quartzite-Amphibolite Complex.

The Jamba Group is found at the Cassinga Zone (Carvalho et al., 2000), to the east of the studied zone (Fig. 2). This group consists of an Archaean volcano-sedimentary sequence with BIF layers, scarce calcareous rocks and clastic sediments (Kopershoek, 1970; Carvalho, 1972, 1981; Bassot et al., 1981; Alkmim and Martins-Neto, 2012). The Jamba Group is configured in NNE-SSE to N-S oriented mega-syncline and anticline folded structures (Kopershoek, 1970; Carvalho, 1982; Bassot et al., 1981, Silva, 2005), whose outcrops extend in the provinces of Matala, Jamba and Cassinga in Angola (Fig. 2).

To the north of the KC, between the voluminous Palaeoproterozoic igneous basement, and scarcely to the west among the outcrops of the Schist-Quartzite-Amphibolite Complex, occurs the Gneiss-Migmatite-Granite Complex (Fig. 2). This metamorphic complex is mainly composed of igneous-derived gneisses and migmatites, together with some metasedimentary lithologies, and represents the Archaean (2.7–2.6 Ga; Delhal et al., 1975; Carvalho, 1982) to Palaeoproterozoic portions amalgamated during the Eburnean Orogeny to conform the Congo Craton, (Cahen et al., 1984; Araújo et al., 1988; Carvalho and de Alves, 1990; De Waele et al, 2008).

The Schist-Quartzite-Amphibolite Complex, occurring to the west of the KC (SQA in Fig. 2), is a large Archaean to Palaeoproterozoic metasedimentary unit structured in a NW-SE-trend (Carvalho and de Alves, 1993; Silva, 2005), that discordantly overlays the Gneiss-Migmatite-Granite Complex. It is constituted by a flysch sequence of low metamorphic degree, mainly composed of schists and greywackes with intercalations of amphibolite and marble layers (Carvalho and de Alves, 1993; Silva, 2005; Pereira et al., 2013a, 2013b).

2.2. The Palaeoproterozoic basement

Between central Angola and northern Namibia, the Palaeoproterozoic crystalline basement is mainly composed of igneous rocks generated during the Eburnean orogeny (e.g., Carvalho, 1982; Silva, 2005; Kröner et al., 2010, 2015; Pereira et al., 2013b, Jelsma et al., 2018). This Palaeoproterozoic igneous basement is usually divided in three major groups of magmatic rocks (Fig. 2; Carvalho, 1982; Pereira et al., 2013b): i) the Gabbro-Diorite Complex, composed of mafic to intermediate (gabbros, diorites, quartz-diorites and granodiorites) and scarce ultramafic materials (dunites, hornblendites, pyroxenites); ii) the Regional Granite (Gr), that includes mainly different calc-alkaline granite lithotypes (granodiorites, monzogranites and syenogranites), together with subordinate rhyodacite volcanic to subvolcanic cogenetic members; and iii) late- to post-Eburnean leucogranites, associated to the partial melting of ortho- and paragneisses, that intruded during the late-stages of the Eburnean orogeny (Pereira et al., 2013b).

To the north and the west of the KC, in the Central Eburnean Zone and the Lubango Zone (Carvalho et al., 2000; CEZ and LZ in Fig. 2, respectively), the Palaeoproterozoic basement is represented by a set of granitoids and sub-volcanic rocks that consolidated between 2.04 and 1.80 Ga (Delor et al., 2006; Pereira et al., 2011, 2013b; Jelsma et al., 2011, 2018; McCourt et al., 2013). On the other hand, the southern KC margin is limited by the granitoid gneisses from NW Namibia, ascribed

to the Epupa Metamorphic Complex, that present U-Pb zircon protolith emplacement ages ranging from 1.86 to 1.76 Ga (Kröner et al., 2010).

The late-Eburnean (Pereira et al., 2011; McCourt et al., 2013) to Mesoproterozoic (Carvalho 1969; Torquato and Salgueiro, 1977; Kröner and Rojas-Agramonte, 2017) metavolcano-sedimentary sequence of the Chela Group constitutes one of the highest mountain ranges in south-central Angola, separating the Huíla Plateau of the interior from the low-lying coastal Namib Desert (Figs. 1, 2, 3). The Chela Group consists of low-grade siliciclastic facies interbedded with volcanic and volcanoclastic materials, with scarce carbonates at the top of the sequence (Carvalho, 1982; Pereira et al., 2011, 2013b; McCourt et al., 2013), deposited as subhorizontal beds over the gneissic and granitic basement from the Lubango area southwards to the Oncocua region (Fig. 2). This group is intruded by Mesoproterozoic red granites of ca. 1.3 Ga and dolerites from 1.5 to 1.1 Ga (Silva et al., 1973; Carvalho et al.; 1987; Ernst et al., 2013).

2.3. The Mesoproterozoic Kunene Complex and related rocks

The Kunene Complex (KC) is an extensive NNE-SSW-trending igneous massif of essentially anorthositic nature, with scarce troctolite, gabbro and norite bodies (Carvalho and de Alves, 1990; Drüppel et al., 2007; Maier et al., 2013). The Kunene Complex intruded over a wide time span during Mesoproterozic times (1503–1375 Ma; Baxe, 2007; Drüppel et al., 2007; Brower, 2017; Bybee et al., 2019), into Archaean to Paleoproterozoic granite-gneiss basement rocks, to the northern and western edge, and into Paleoproterozoic metamorphic rocks of the Epupa Complex, to the south. Slightly older to coeval granite bodies, composed of "Red granites", rhyolites, leucogranites, quartz-monzonites, syenites and other related volcanic felsic rocks, intruded in association to the KC (Mayer et al., 2004; Baxe, 2007, McCourt et al., 2013; Kröner and Rojas-Agramonte, 2017; Brower, 2017).

Massive anorthosites constitute about 90% of the exposed volume of the Kunene Complex; in most cases, are unaltered, and preserve primary igneous textures, i.e. with lack of metamorphic overprint (Slejko, et al. 2002). Nevertheless, solid-state metamorphic structures are found at different parts of the massif, consisting of alternating anorthosite members showing unaltered and metasomatized textures (named as black and white anorthosites; Morais, et al., 1998; Drüppel et al., 2007; Bybee et al., 2019). They, occasionally, show ductile deformational structures, which lead Lehmann et al. (2020) to relate the KC intrusion to a compressional regime. The intrusive contacts of the Kunene Complex with the host rocks tend to be modified by ductile NNE-SSW-trending shear zones at the western edge (Lehmann et al., 2020), except for some outcrops far south in the Zebra Mountains (Namibia), which shows an elongated highly tectonized E-W-trend. The eastern segment of the massif is completely covered by Cenozoic sediments of the Kalahari Group (Fig. 2), and no information of this area has been provided up to date.

Distinct Mesoproterozoic mafic intraplate events have been recorded in SW Angola, between 1502 ± 5 Ma (obtained in a dolerite sill intruding into the Chela Group in the Humpata region), 1200 Ma (K-Ar dating in NW-SE-trending dolerite dykes or subhorizontal sills from the Oncocua region; Silva et al., 1973; Carvalho et al., 2000) and 1110 ± 3 Ma (in a gabbronorite dyke below the Chela Group, related to the N-S-trending family of dyke swarms of southern Angola), interpreted as part of the plumbing system of LIPs (Ernst et al., 2013; Salminen et al., 2018). The intrusion of these dolerite dykes probably took place all over Angola favoured by regional fracturing and reactivation of older structures (Andrade, 1962). The gabbronoritic dykes (~1.1 Ga) constitute the last mafic magmatic extensional event that promoted the rupture of the Nuna/Columbia Supercontinent (Meert, 2012; Pereira et al., 2011; Ernst et al., 2013; Evans 2013; Silveira et al., 2013). This intraplate magmatic event is coeval in Congo and San Francisco Cratons and support their connection during the Mesoproterozoic (De Waele et al., 2008) previous to their Early Neoproterozoic continental break-up (Schannor et al., 2019).

2.4. The Pan-African orogeny

The Pan-African Orogeny occurred from 870 to 520 Ma (e.g., Kröner and Stern, 2005; Goscombe et al., 2017), where a number of mobile belts were formed as a consequence of remobilisation of older cratons. The Angola Shield, assembled to the Congo, São Francisco and Kalahari Cratons during Neoproterozoic times, is surrounded by the West Congo Belt to the north, in a NW-SE trend; the Lufilian Arc to the east; and the Damara Belt to the south. The connection between these belts is still a matter of debate, since their prolongation is hidden beneath the Cenozoic cover. The Pan-African NNW-SSE Kaoko Belt is well exposed in southwestern Angola and NW Namibia (Figs. 1 and 2). Its prolongation towards the north and its relation to the Aracuai-Ribeira Belt is commonly suggested, being mostly located in the Brasilian coastal margin after the Gondwana breakup (e.g., Kröner and Correia, 1980; Kröner and Stern, 2005; Hanson, 2003).

2.5. The Mesozoic to Cenozoic Atlantic rifting and the filling of intra-continental basins

The Post-Permian geology of SW Angola links to the Gondwana breakup and the opening of the Atlantic Ocean. The continental rifting in Angola begins in the Cretaceous, at pre-Aptian times (Brognon, 1965; Pereira, 1971; Marsh and Swart, 2018). This geological record consists of marine sedimentary and magmatic rocks formed during the Meso-Cenozoic Atlantic opening, including olivine basalts, latites, basanites and teschenites (Marzoli et al., 1999; Marsh and Swart, 2018), occasionally interbedded within the sedimentary units, cropping out mainly in the northwestern studied area (Fig. 2). At the end of the Cretaceous, followed a strong cycle of tectonic uplift and intracontinental subsidence during which the regional relief was highly eroded (Pereira, 1977). The formation of distinctly elevated crustal portions promoted the generation of intra-continental basins and the region was covered by thick sedimentary mud-sand-conglomerate sequences of the Kalahari Group. In Angola, the Kalahari sediments accumulated throughout the entire Cenozoic forming the Kalahari basin (Matmon et al., 2015), covering almost the entire eastern part of the country, including the eastern edge of the Kunene Complex (Fig. 1 and Fig. 2).

3. Bouguer anomaly map

The Bouguer anomaly gridded data used in this study covers an area of 7° x 4° NS and WE, and was obtained from the Bureau Gravimetrique International database (Bonvalot et al., 2012). The regional Bouguer gravity anomaly grid (in geographic coordinates in decimal degrees on a 2.5′ x 2.5′ grid) are computed at BGI from the EGM2008 spherical harmonic coefficients (Pavlis et al., 2008). The Bouguer corrections computed at regional scales are obtained using the FA2BOUG code developed by Fullea et al. (2008). The topographic is computed at the Earth's surface (lower limit of the atmosphere) with a 1′x1′ resolution and the correction is applied up to a distance of 167 km using ETOPO1 Digital Elevation Model (Amante and Eakins, 2009). The reference density used for the Bouguer is 2.67 g/cm^3. The EGM2008 model includes surface gravity measurements (from land, marine or airborne surveys) and satellite altimetry and satellite gravimetry (GRACE mission) measurements, where topography corrections are applied. In this case, the available ground data are so few that the satellite data are the dominant source of information providing a uniform coverage in the area. The satellite gravity data over Angola is of particular value, since more detailed private sector ground and airborne data would be sparse for such a cortical study.

The selected area is located from the northwest coastline of Namibe to the Caiundo town in the east and northern Matala town (longitude 11° to 18° East and latitude 14° to 18° South; Figs. 1 and 2). In order to work with projected coordinates, we converted the geographic coordinates to UTM using the WGS84 datum, Zone 33S. The complete

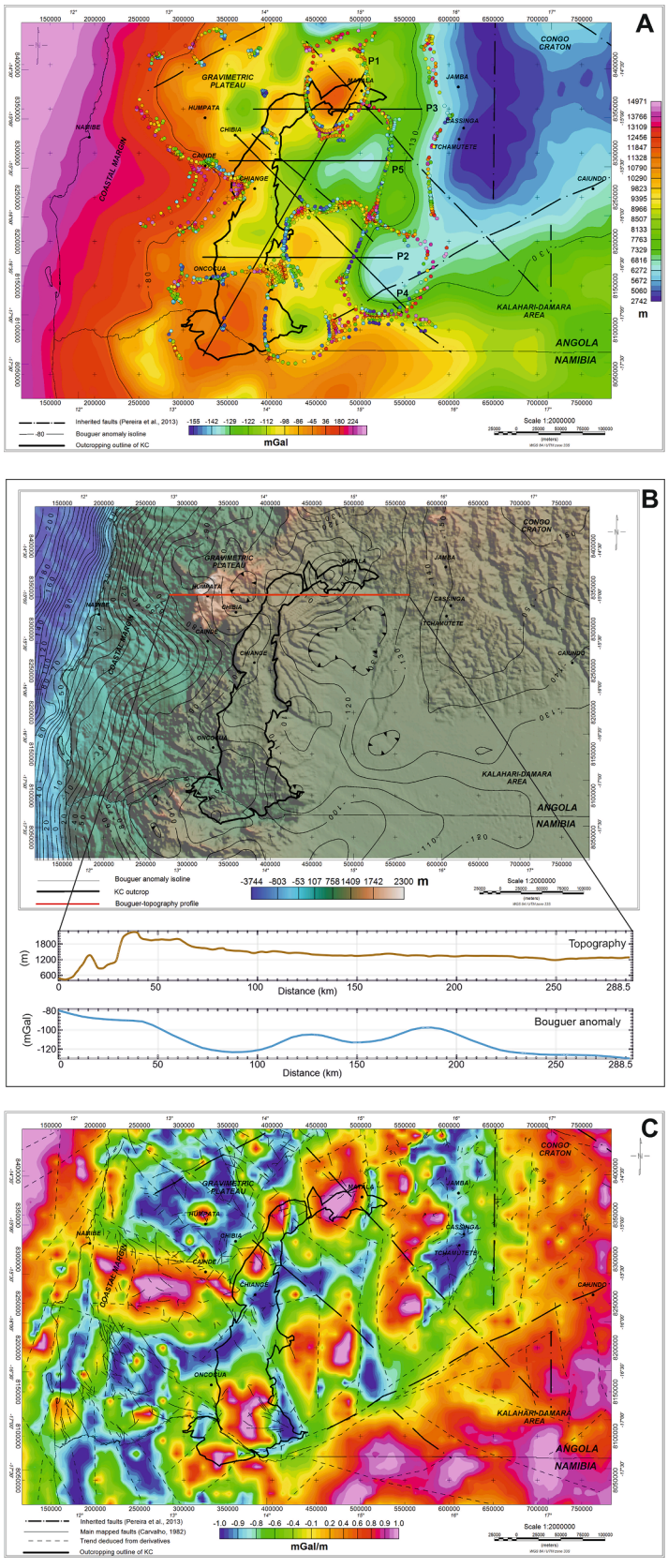

Fig. 3. A) Bouguer anomaly map with the three delimited areas: coastal margin (red colours), gravimetric plateau and Kalahari area (orange to green) and Congo Craton (blue). The limit of the outcropping KC is shown (black thick line) and the five 2.5D modelled profiles (P1, P2, P3, P4 and P5). The main faults according to Pereira et al, 2013a, 2013b (NW-SE, NE-SW and N-S, black dashed-dotted lines) are shown. Euler deconvolution solutions (SI = 0) coloured circles represent Euler solution depths. B) Topographic map (ETOPO1 Digital Elevation Model -Amante and Eakins, 2009) overlaid with the Bouguer anomaly isolines. The Bouguer-topography profile helps to unravel the contribution of the topography to the Bouguer anomaly. C) Generalised derivative of Bouguer data. Overprinted inherited faults (black dashed -dotted line) are from Pereira et al. (2013a, 2013b), whereas the mapped faults (black solid thin lines) are from Carvalho (1982). The distinct trends (black dashed line) are deduced from the generalized derivatives. Outcropping KC in thick solid line. See text for further discussion.

Bouguer anomaly map of the studied area is gridded with the minimum curvature method, has a cell size of 5000 m and a low-pass desampling factor of 3 was applied, which effectively act as a smoothing filter by averaging all points into the nearest cell defined by the factor (Fig. 3A). The map covers an area of about 282000 km^2 and depicts an anomaly range from positive values on the Atlantic coast (> +225 mGal) to negative values towards the northeast (<-150 mGal). The gradient that varies along 600 km in an E-W trend can be explained by large-scale variations in the crust (e.g. undulations at crustal scale, variations between upper and lower crust) and by the distribution of subcontinental lithospheric mantle (SCLM) as pointed by Begg et al., 2009. It represents the transition from a younger dense basaltic and thin oceanic crust, formed during the Mesozoic Atlantic rifting, to an older lighter and thicker continental crust (Congo Craton) to the east (Nicolai et al., 2013).

By comparing Bouguer anomaly data with digital elevation data the reliability/quality of Bouguer anomalies can be checked, as the topography can contribute to some of the anomalies. The topographic map (Fig. 3B, ETOPO1 Digital Elevation Model -Amante and Eakins, 2009) is gridded at a cell size of 500 m with a range from −3074 m at the west (Atlantic Ocean) to + 2300 m around Humpata and Chibia towns. An analysis of the wavelengths contained in the data is done by comparing high frequency variations with the topographic data that helps to clarify the topographic corrections. We choose one W-E profile (Fig. 3B) running from west Humpata (580 m elevation), the Chela Planalto (2300 m elevation) ending west of Cassinga (1200 m elevation) along 288.5 km, representing a good example to evaluate both gravity and topographic data. The Bouguer anomaly data ranges from −80 mGal to −120 mGal and in between kilometres 100 and 200 of the profile two relative gravity maxima correspond to an even topography with proves that topography effect does not influence the Bouguer anomaly data.

In order to better define some of the linear features in this regional context we use the curvature of the potential field response to enhance the signal and increase the lowest amplitude anomalies (<50 km). Explicitly, we use here the generalized derivative, which is a filter of a linear combination of the horizontal and vertical field derivatives (Fig. 3C), normalized by the analytic signal amplitude (Cooper and Cowan, 2011). Other regional lineaments (mostly brittle fractures) have been extracted from the literature (Carvalho, 1982; Pereira et al., 2013b). As can be shown in Fig. 3C, the design of the structural trends is based on the first-order changes suggested by the distinct responses of the Bouguer derivatives, in addition to other minor contrasts, which clearly evidence the structuring of the crystalline basement. In fact, on the western margin of Angola, NW-SE trends are evident, which would be related to the structuring of the Schist-Quartzite and Amphibolite Complex, while NNW-SSE to NNE-SSW trends would probably be associated with the crustal remobilization reached during the Pan-African. Other some major NE-SW, NW-SE and N-S trends could be related to extensional Mesoproterozoic structures, probably reactivated during the Mesozoic Atlantic rifting and subsequent continental drifting. Other minor N-S trends found in the central region of the studied area would be associated to the KC intrusions, to brittle and linear structures related to the distinct dolerite and gabbro-norite dykes and even to the structure of the Archaean basement in the Cassinga area, as seen in the topographic and drainage pattern of this region (Fig. 3B).

In the Bouguer anomaly map, four major gravimetric zones have been differentiated (Fig. 3A) based on the values of the Bouguer anomaly: 1) Over −80 mGal, named as coastal margin, red colours. 2) Between −80 and −130 mGal, intermediate values of Bouguer anomaly that responds to long – medium (40–60 km) wavelengths, designated as the gravimetric plateau, in orange-green colours. 3) Below −130 mGal that include lower values and wavelength between 50 and 60 km, in blue, noted as the Congo Craton gravity area. 4) Kalahari-Damara, at the southeaster corner limited to the isoline of −100 mGal to the west and −130 mGal to the north. Both the gravimetric plateau and Congo Craton are well defined by Bouguer anomalies and can be included in the Angolan Shield (Jelsma et al., 2018).

A) Coastal margin. This area comprises values over + 80 mGal of Bouguer anomalies (red colours in Fig. 3A). This suggests that the transition from the oceanic crust to the continental crust should occur over a narrow fringe at the coastal line, according to the decrease in the Bouguer anomaly values, with minor complications due to stretching. The gravimetric response of the Post-Permian and the Palaeocene and Pleistocene units together with the granitic-metamorphic complexes remains capped by the gravimetric long wavelength anomaly (greater than 100 km), that corresponds to the dense oceanic crust located to the west. This unit is structured in a NNE-SSW trend, showing a conjugated system of NW-SE to NE-SE transcurrent faults (see major trends in this area in Fig. 2 and Fig. 3C), mainly related to the geometry of the opening margin of the Atlantic Ocean and subsequent drifting (Pérez-Díaz and Eagles, 2014). These structures were probably reactivated during Mesozoic to Cenozoic times, taking advantage of other previous structures generated during earlier (mainly Proterozoic) tectonic events (Torquato, 1977).

B) Intermediate gravimetric plateau, from orange to green colours (Fig. 3A). In this extensive area a set of maximum and minimum anomalies with wavelengths between 40 and 60 km associated to density contrasts between Palaeoproterozoic metasedimentary and igneous - lithologies and Archaean to Palaeoproterozoic metamorphic complexes remobilized during the Eburnean event (Carvalho, 1982). Wider wavelength anomalies seem to be produced by mafic KC materials in the Matala and Oncocua regions. The south responses extend to the Namibian lobe of KC (Zebra Mountain ranges), which gravimetric response seems to copy the pattern of mafic intrusions (Ashwal, 1993). The western limit of the outcropping KC (see Fig. 3A, black line) seems to delineate a set of relative gravity maxima (-90 mGal), serving as proxy to evaluate the KC influence in the gravimetric record. These patterns are in concordance with the residual Bouguer anomaly map of Africa, obtained by Braitenberg (2015). A similar anomaly pattern is observed in both works, with a relative maxima subparallel to the coastline in the SW corner of Angola (Braitenberg, 2015 and this paper). A robust relative maxima anomaly of ~ 30 mGal is presented in the interior of Angola in a large-scale African residual Bouguer map (Braitenberg, 2015), an area where our work differentiates certain relative maxima of the Bouguer anomaly of ~ -45 mGal, which would be related to the KC (Fig. 3A). On the other hand, eastward of the KC outcrops, the anomaly decreases, being difficult to unravel its prolongation under the Kalahari sediments. To the north, in the Matala area, the relative gravity maxima are related to the metasomatized gabbros from the Kunene Complex that crop out in the field (Carvalho, 1982), suggesting a wider extent underneath. Related derivatives (Fig. 3C) present N-S and NE-SW trends in this area, possibly as a result of the Eburnean tectono-metamorphic processes and the distinct Mesoproterozoic (±Meso-Cenozoic) extensional events. In fact, Lehmann et al (2020) detect steep N-S striking foliations in footwall anorthosite and porphyritic granite concordant with fold axial planar leucosomes and gneissosity in the central Angola basement.

C) Congo Craton. Toward the east, the Bouguer anomaly map records the lowest values (below −130 mGal), where a broad extension of Paleocene-Pleistocene materials covers the basement rocks. Global seismic tomographic imaging shows that significant parts of Congo Craton extend to depths of greater than 300 km (Begg et al., 2009), corresponding to the northeastern area of this work. In this zone, the Archaean to Palaeoproterozoic units (reworked during the Eburnean, see geological map of Fig. 2) do not display specific gravity responses within the minimum gravity anomaly that characterizes this region. The derivatives

(Fig. 3C) point to some N-S trends, possibly associated with the Archaean to Paleoproterozoic structure of this region, or even with crustal fracturing related to the intrusion of the late-Mesoproterozoic N-S gabbronorite dykes.

D) Kalahari-Damara area. This zone is located at the SE border of the studied zone and encompasses an area covered mainly by Paleocene to Pleistocene deposits from the Kalahari Group. The gravity depicts relative gravity values ranging between −100 and −130 mGal. The Kalahari deposits record the most recent geological history of southern Africa, with evidence of a complex history of reactivation of older structural orientations or weakening over time (Haddon, 2005). In fact, this area is bounded to the north with the Congo Craton by a large ENE-WSW oriented structural lineament from Caiundo to the southwest (Pereira et al., 2013b). Moreover, this lineament is drawn with the derivatives by a large set of NE-SW trends (Fig. 3C). In line with the pervasive trend within the Damara belt, this orientation could be associated with Pan-African structures (delineating roughly the northern foreland Damara limit), or other structures inherited from the Proterozoic. In any case, this crustal structure seems to be responsible for the topographic modelling and drainage patterns of this region (Fig. 3B).

4. Petrophysics

For the geophysical models, statistic average densities (considering their standard deviation) were assigned to quantify their relative contributions to the observed regional Bouguer gravity signal (Tables 1 and 2). Due to the non-uniqueness of potential-field data modelling, i.e., multiple models can satisfy the observed gravity field, important information can be retrieved from the 2.5D modelling about the subsubsurface, in particular if geological, drill-hole or other geophysical information is available. In this study, the only available information was mapped units and density data to constrain the modelling. For 2.5D modelling, the spatial configuration of the bodies is constructed based on the physic properties of the materials, in this case the density contrast of the rocks involved. Moreover, such configuration must respect the geological features and additional direct and indirect survey data. The mapped geological units, discontinuities and mapped structures are therefore the main conditioning factor of the model, respecting the density values measured or consulted in the literature. The processing of data, such as Euler depths, or the calculation of the derivatives presented in this work, help us to understand how deep features could be expressed when covered by recent rocks.

The main premise of this study is the interposing positive anomaly by

Table 1
Sample label, volume of rock (if known), density, method used for determining the density measurements, and lithology of the 38 rock samples from the regions of Tchamutete and Chiange (see Fig. 2 for location), with mean and standard deviation for the different lithological types. The scale provides sensitivity to two decimals of a gram while the helium picnometer provides sensitivity to four decimals of a gram.

Sample	Volume (cm^3)	Density (g/cm^3)	Method	Lithology
				Tchamutete town
BASE1	5.3143	2.64	Helium pycnometer	Phyllites. White and pink metagreywackes,quartzites and matapelites
BASE2	6.0932	2.66		
BASE3	13.766	2.75		
TCH2-1	7.0347	2.80		
TCH2-2	12.5604	2.64		
TCH2-3	13.764	2.64		
TCH2-4	13.3957	2.70		
TCH2-5	41.7	2.61	Hydrostatic balance	
Mean: 2.68 g/cm^3 Std DV: 0.065247				
				Chiange town
CHI5-1	8.16	2.81	Water displacement (volume) and weight	KC Gabbros
CHI5-2	6.46	2.80		
CHI5-3	6.51	2.81		
CHI5-4	8.6	2.80		
CHI5-5	6.14	2.81		
Mean: 2.81 g/cm^3 Std DV: 0.005478				
				East of Chiange town
357A-052		2.78	Water displacement (volume) and weight	KC Anorthosites
357A-055		2.79		
357A-062		2.78		
357A-064		2.75		
357A-066		2.83		
357C-023		2.77		
357C-040		2.69		
357C-041		2.74		
357C-042		2.76		
357C-043		2.80		
357C-050		2.79		
357C-052		2.75		
357C-06		2.76		
378-A-001-M−001		2.71		
378A-021		2.82		
378A-022		2.76		
378A-025		2.75		
378A-026		2.83		
378A-027		2.73		
378A-028		2.67		
378A-032		2.63		
378-C-006-M−006		2.67		
378-C-001-M−001		2.70		
378-C-002-M−002		2.76		
378-C-004-M−004		2.77		
Mean: 2.75 g/cm^3 Std DV: 0.050718				

Table 2
Density values used in the modelling of the five profiles. Code labelling and colour employed in the models. Lithology of the body. Density (g/cm^3), with associated reference, and cronoestratigraphy of each unit. (See below-mentioned references for further information.)

Code	Lithology	Density (g/cm^3)	Std DV	Source	Chronostratigraphy
S-c	Sands and clays	2.0		Johnson & Olhoeft, 1984	Pleistocene-Paleogene
S	Sands	2.5		Johnson & Olhoeft, 1984	Pleistocene-Paleogene
gr	Red granites and rhyolites	2.65		Finn et al., 2015	Mesoproterozoic Kibaran
KC-gb	Metasomatized gabbros	2.81	0.005478	This work	
KC-an	Anorthosites	2.75	0.050718	This work	
d	Olivine dolerites	2.70		Johnson & Olhoeft, 1984	
Ch	Quartzites & metavolcanoclastic rocks. Chela group	2.68		Johnson & Olhoeft, 1984	Palaeoproterozoic
Gr	Granitoids	2.65		Finn et al., 2015	Palaeoproterozoic-Eburnean
Gr-grn	Granodiorites & quartz-diorites	2.68			Palaeoproterozoic-Eburnean
N-gb	Noritic gabbros	2.85		Sharma et al., 1997	Palaeoproterozoic-Eburnean
Bs	Metasedimentary and igneous derived materials	2.67		Nafe & Drake, 1957; Barton, 1986; Rudnick & Fountain, 1995	Neoarchaean
M-C (Middle Crust)	Undifferentiated amphibolite and granulite facies metamorphic materials	2.80		Lowrie, 1997	Archaean

the KC bodies with regard to the descending gradient Bouguer anomaly map encountered from coastline to hinterland terranes, to verify the KC extension to the east under the young sedimentary cover. Density data were assembled using unified modelling, where the density field data is used to constrain the forward 2.5D modelling. Unified modelling is so called when petrophysical data are implemented with real data and serve to constrain geophysical modelling. Uncertainties involved in 2.5D modelling would be therefore be the extension and depth of the KC bodies, the geometrical configuration of such bodies and the density properties of modelled bodies. To reduce the uncertainties individual samples were obtained from assorted outcrops and cut to avoid weathered surfaces. Measurement of density of outcrop samples obtained from the study area with sufficient statistical representativeness provide a reduction of uncertainties in the modelling process.

25 anorthosite samples were available from the study area (kindly provided by PLANAGEO project) and another 13 samples (metasedimentary rocks and gabbros) obtained from the Zaragoza University (personal communication), from former projects, from which we could obtain certain amount of original density values (Table 1 for location). All measured samples were collected from fresh outcrops, with no evidence of alteration. Table 1 contains the density and methods used of some lithologies coming from the KC, which have been used in 2.5D gravity modelling in this work. The helium pycnometer was used in anticipation of dealing with porous rocks for which an open porosity measurement was devised. Ten measurements were made to achieve a mean with a standard deviation of ± 0.001 g, obtaining an average density of ± 0.0005–0.005 g/cm^3. On the other hand, crystalline rocks, such as gabbro and anorthosite, where no significant open porosity was expected, were measured by the quickest and most accessible method, water displacement and weight. Two repetition of the measurements were carried out, observing a variation in measurement of one hundredth of a gram.

The lack of field measurements of host rocks makes it necessary to use worldwide-recognized reference density data (Telford, et al. 1976), equivalent to the outcropping rocks, and empirical relationship between crustal P waves/density, as explained Nafe and Drake, 1957, Barton, 1986, Rudnick and Fountain, 1995. A summary of the field and reference density data used in the modelling is shown in Table 2. The density of the samples measured in the laboratory (Table 1) is included in Table 2, whose density values have been used for modelling.

In summary, the petrophysical data shows the following standard densities: the densest rocks are related to gabbros, (2.81 g/cm^3) from KC, Eburnean noritic gabbros (2.85 g/cm^3) and the units from middle-crust (2.80 g/cm^3) (Table 1 and 2); olivine dolerites (2.70 g/cm^3) and anorthosites (2.75 g/cm^3, Table 1) represent medium–high values of density. Medium-values correspond to metasedimentary and igneous derived materials, granodiorites & quartz-diorites, and quartzites & metavolcanoclastic (2.67–2.68 g/cm^3) (Table 2), whereas the least dense rocks are represented by red granites and rhyolites, granitoid rocks and sands (2.0–2.65 g/cm^3, Table 2). The contrast expected

between the KC bodies, including gabbros, anorthosites and red granites, intruded in Mesoproterozoic Kibaran episodes and the Archaean host rocks, as well as Proterozoic Eburnean rocks, deliver to the starting premise, allowing a more reliable determination of the configuration of the bodies involved. Addressing this point, we have tested some different configuration of bodies involved in modelling (see Supplementary Figs. 1, 2 and 3) and some variation in density (within the standard deviation of the gabbros and anorthosites, see Table 1). Considering the regional study, the difference in density between Archaean host rocks and KC bodies (2.67 g/cm^3 *vs* 2.75–2.81 g/cm^3) would be enough to decipher depth and morphology of the KC. A certain degree of uncertainty is assumed associated with the petrophysical characterization carried out, as well as with the expected densities of some lithologies, that change significantly with depth. Nevertheless, the standard deviation for the measured units provides reliability of the data (Table 1).

5. Euler solutions

Euler Deconvolution is a method of grid analysis, firstly developed by Thompson (1982), to make depth estimations from large amounts of magnetic data. Nevertheless, this technique, based upon Euler's homogeneity relationship, is also applied to gravity methods (Keating, 1998), as demonstrated on the Bouguer anomaly, according to the equation (Thompson, 1982):

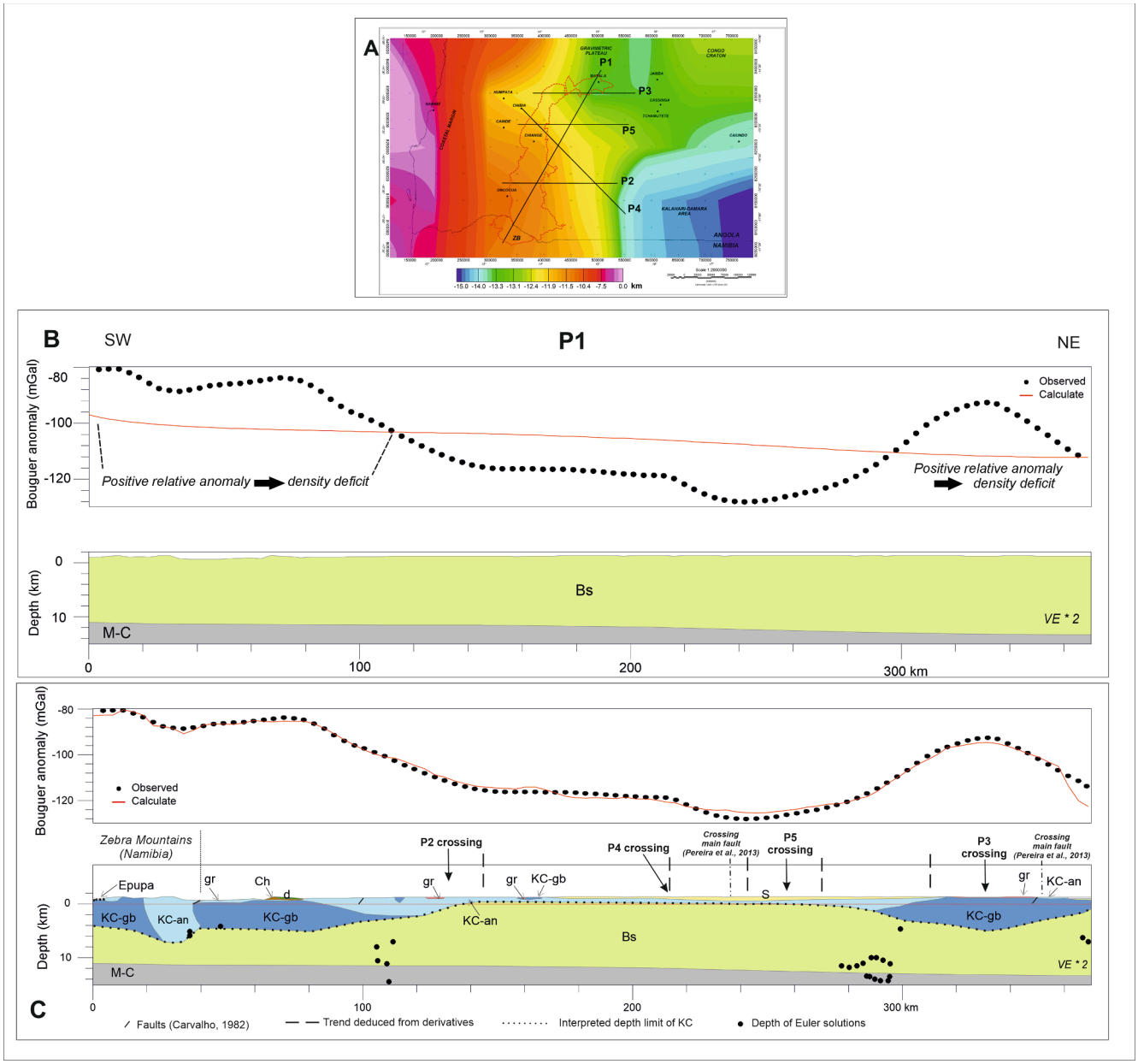

Fig. 4. A) Location of the profiles on the map displaying Middle Crust (M−C) and the Basement (Bs) boundary (extracted from Laske et al., 2013). B) Crustal model representing the Middle crust and Basement boundary, where deficit or excess of density is observed. C) Bouguer anomaly fitting by the model of the Profile 1 (see Figs. 2 and 3A for location), of 370 km long, by means of bodies which configuration is interpreted as follows: Middle Crust (M−C) and Basement units: Metasedimentary and igneous derived (Bs), Neoarchaean, intruded by KC (anorthosite, KC-an, and gabbro, KC-gb) and red granites (gr) during the Mesoproterozoic. Sediments of Chela group (Ch) and dolerites (d), in the Palaeoproterozoic, crop out at km 80. In Neogene times, Kalahari units (S) would be sedimented as northeastern outcrops (Fig. 2). Euler solutions are shown in depth. Pointed line represents the interpreted depth limit of KC in this work. The crossing of profiles P2, P4, P5 and P3, main faults (Pereira et al., 2013a, 2013b) and trends deduced from derivatives are depicted throughout the profile trace. Vertical exaggeration 2.

$$(x-x_0)\frac{\partial T}{\partial x}+(y-y_0)\frac{\partial T}{\partial y}+(z-z_0)\frac{\partial T}{\partial z}=N(B-T)$$

Where T is the observed field; X_0, Y_0, Z_0 are source anomaly locations; B is the base level of the observed field; and N is a structural index. This equation is used to solve equation systems over a moving window, optimized by clustered solutions with a small relative error. This technique serves to determine different sources of anomalies caused by density contrast, and estimate their depths. We use it in this work as an additional methodology to support our 2.5D modelling. Fig. 3A shows the Euler's deconvolution solutions over the selected area of 140000 km^2. Following the guidelines detailed in Reid et al. (2014), the selected window size is 50000 m (ten times the grid spacing) that provides shallower and deeper solutions. In practice, this technique is most effective in characterizing dykes, sills, normal faults or other lateral changes in density, so we choose a structural index (SI) equivalent to 0 (resembling thin sheet edge, thin sill and thin dyke for gravity, after Reid et al., 2014). We assume it will represent better the density contrast boundaries between different bodies at this regional scale. Structural index 1 and 2 were discarded because they do not help to define subvertical boundary geometries, which are the scope of the investigations of the eastern limit of the KC. Euler deconvolution, for the selected area provide a dataset of 2557 solutions and infers source depth solutions ranging from 2.7 to 38.8 km. As our interest is finding the contacts in the Upper Crust we filter the dataset between 2.7 and 15 km obtaining 1679 solutions depicted in Fig. 3A. These solutions will improve the profiles modelled in this work (Figs. 4, 5, 6, 7 and 8). In this regard, the western limit of Euler solutions in the north coincides with the contact between the least dense Regional Granite (Gr) (Fig. 2) and the denser materials (Neoarchaean Complex: gneiss, migmatite, granite), matching with the isoanomaly of – 80 mGal. South to the KC outcrops, some solutions remark the important density variance in the south related to the Zebra Mountains; also in the north, around the Matala region, a high density body is clearly circumscribed by the Euler solutions. To the east, a clear N-S lineation of the solutions is evident at 15° longitude. The Euler solutions, together with the 2.5D profiles, are used to derive the eastern KC boundary under the tertiary sediments (see Fig. 10 and final interpretation in the discussion). The projection of Euler solutions in the modelled profiles (between 0 and 15 km) provide more clarification of deepness and would help to delineate the eastern extension of the KC.

6. 2.5D Modelling. Configuration and interpretation of the gravity models

The modelling of the gravimetric profiles yields a better understanding of the deep architecture of the Kunene Complex by creating a subsurface geological model that fits the response of the Bouguer anomaly. The ultimate goal is to use gravity modelling supported by density properties to interpret the geological context of the KC.

Five 2.5D gravity profiles have been constructed crossing through different directions the SW crystalline basement of the Congo Craton (Fig. 2 and Fig. 3A for location) in order to build geological models of the deep geological structures.

Modelling was processed and analyzed using Oasis Montaj© software, which provided a complete solution for gravity modelling. In this case, we use as constraints the morphology between Middle-Crust - Basement (to adjust the long wavelength regional anomaly), obtained from Laske et al. (2013), and the outcropping units. The geological models built include lithostratigraphic information and structural information (Carvalho, 1982). Regarding the latter, the fractures obtained from Carvalho (1982) seem to be too small to affect the gravity at this scale. Afterward we add the results from Euler deconvolution to the profiles. From now on, we interpret in the Bouguer anomaly map some positive anomalies associated with the gabbroic bodies intruding host rocks. The geometries of the bodies are modified and featured with a unique density property. The density values used are summarised in Table 2. The back-and-forth procedure ends when a geologically reasonable geometry is obtained (see the three supplementary figures for the trial process).

The interpretation of geophysical and geological features, aimed at unravelling the deep geometry of the KC through 2.5D gravity modelling, represents a key element to better understand the emplacement of KC in the Congo Craton in Mesoproterozoic times.

All profiles have projected coordinates: WGS844 UTM zone 33S.

The crustal depth of the studied area is poorly known and only some regional works have been published (see Pasyanos and Nyblade, 2007

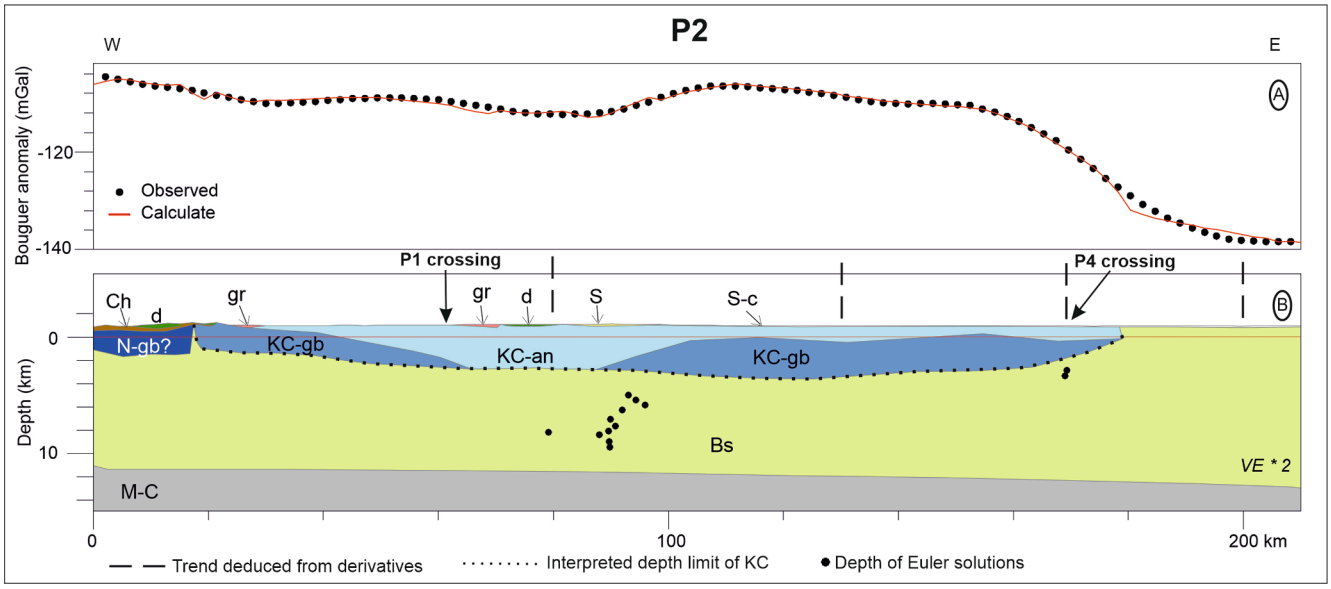

Fig. 5. Bouguer anomaly fitting by the model of the Profile 2 (see Figs. 2 and 3A for location), of 215 km long, is characterized by bodies which configuration is interpreted as: Middle Crust (M–C) and Basement units: Metasedimentary and igneous derived (Bs), Neoarchaean, intruded by noritic gabbros in the west of the profile, during the Eburnean Episode; subsequently overlaying Chela group (Ch) and dolerites (d). KC (anorthosite, KC-an and gabbro, KC-gb) and red granites (gr) intruded during the Mesoproterozoic. Euler solutions are shown in depth. Pointed line indicates the interpreted depth limit of KC in this work. The crossing of profiles P1 and P4, and trend deduced from derivatives are shown. Vertical exaggeration 2.

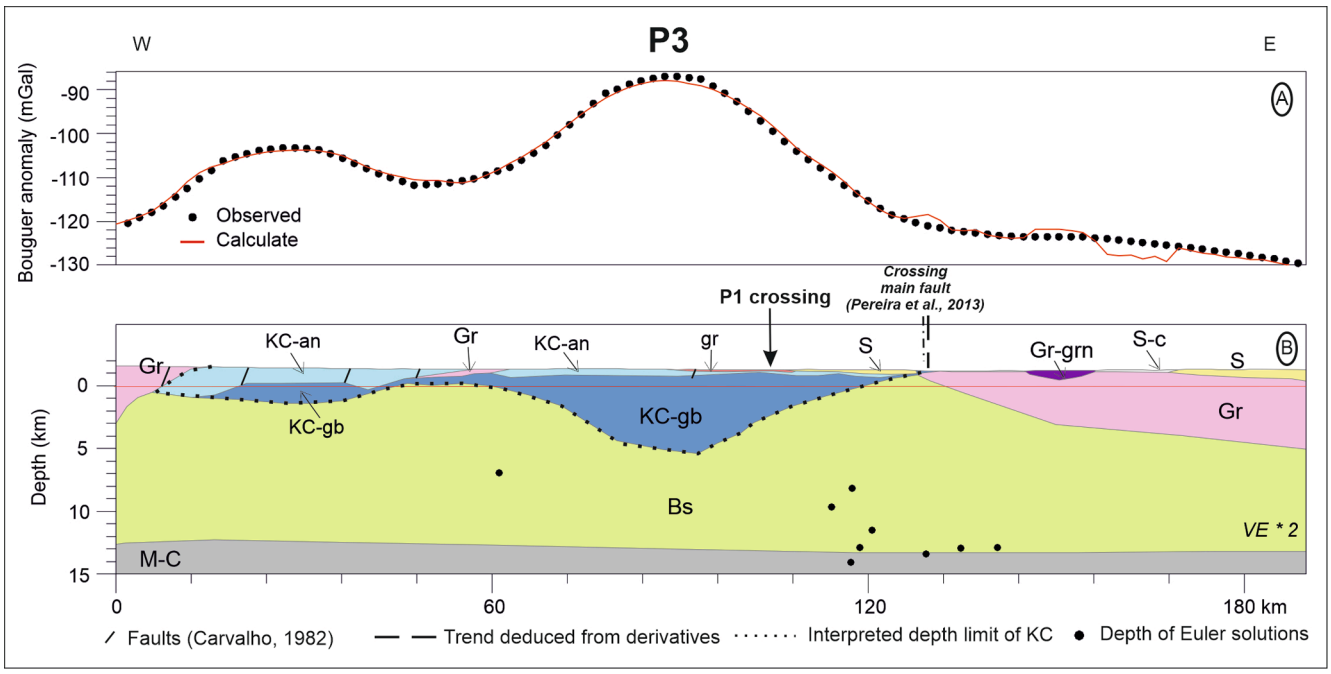

Fig. 6. Bouguer anomaly fitting by the model of the Profile 3 (see Fig. 2 and Fig. 3A for location), of 190 km long, is characterized by bodies which configuration is interpreted as: basement units (Bs): Metasedimentary and igneous derived, Neoarchaean, intruded by eburnean Regional Granite (Gr). During Mesoproterozoic emplaced the KC (anorthosite, KC-an, and gabbro, KC-gb) and red granites (gr). In Neogene times, Kalahari units (S and S-c) would be sedimented at small basins (Fig. 2). Euler solutions are shown in depth. Pointed line represents the interpreted KC boundary in depth in this work. The crossing of main faults (Pereira et al., 2013a, 2013b) and one trend deduced from derivatives are depicted that coincide with the easternmost extension of KC. Vertical exaggeration 2.

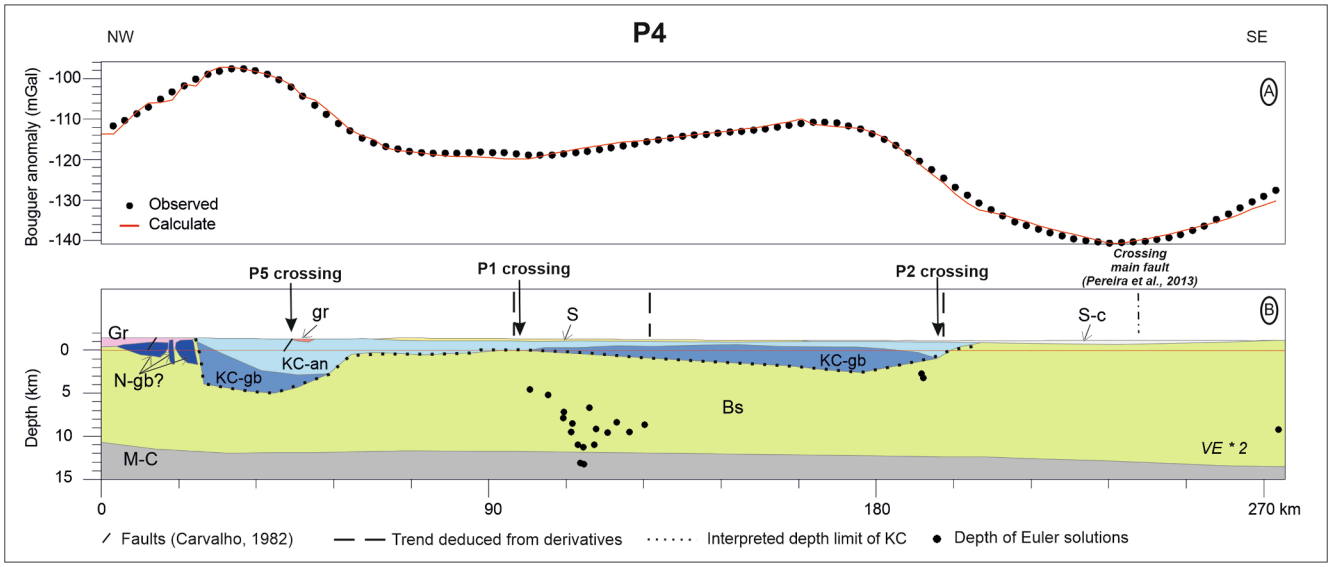

Fig. 7. Bouguer anomaly fitting by the model of the Profile 4 (see Figs. 2 and 3A for location), of 274 km long, which bodies' configuration is interpreted as Middle Crust (M−C) and Metasedimentary and igneous derived, Basement (Bs), Neoarchaean, intruded by noritic gabbros (N-gb) and Regional granite (Gr) during the Eburnean episode. Post-tectonic KC (anorthosite, KC-an, and gabbro, KC-gb) and red granites (gr) emplaced during the Mesoproterozoic. In Neogene times, Kalahari units (S and S-c) would be sedimented (Fig. 2). Euler solutions are shown in depth. Pointed line represents the interpreted KC boundary in depth in this work. See the crossing of profiles P5, P1 and P2, and some trends deduced from derivatives. The crossing of main faults (Pereira et al., 2013a, 2013b) coincides with the thickening of the Basement. Vertical exaggeration 2.

and references herein; Begg et al., 2009). We use the public data available in https://igppweb.ucsd.edu/~gabi/crust1.html (Laske et al., 2013) to set the limit between the Middle Crust (M−C) and the Basement (Bs), whose values are depicted in Fig. 4A, ranging from 7 km in the coastal margin to 15 km depth in the southeastern corner. In the five modelled profiles, this limit lies between 11 and 13 km deep.

PROFILE 1

The first profile runs from SW (x = 322331; y = 8070510) to NE (x = 506231; y = 8392971), for 370 km (Figs. 2 and 4), revealing a significant area of low density. The outcropping units mainly consist of olivine-bearing dolerites, anorthosites and gabbros (KC), together with some red granites and rhyolites, all of them Mesoproterozoic. Upper Kalahari sands are widely found over these materials at the centre and north-eastern section of the profile.

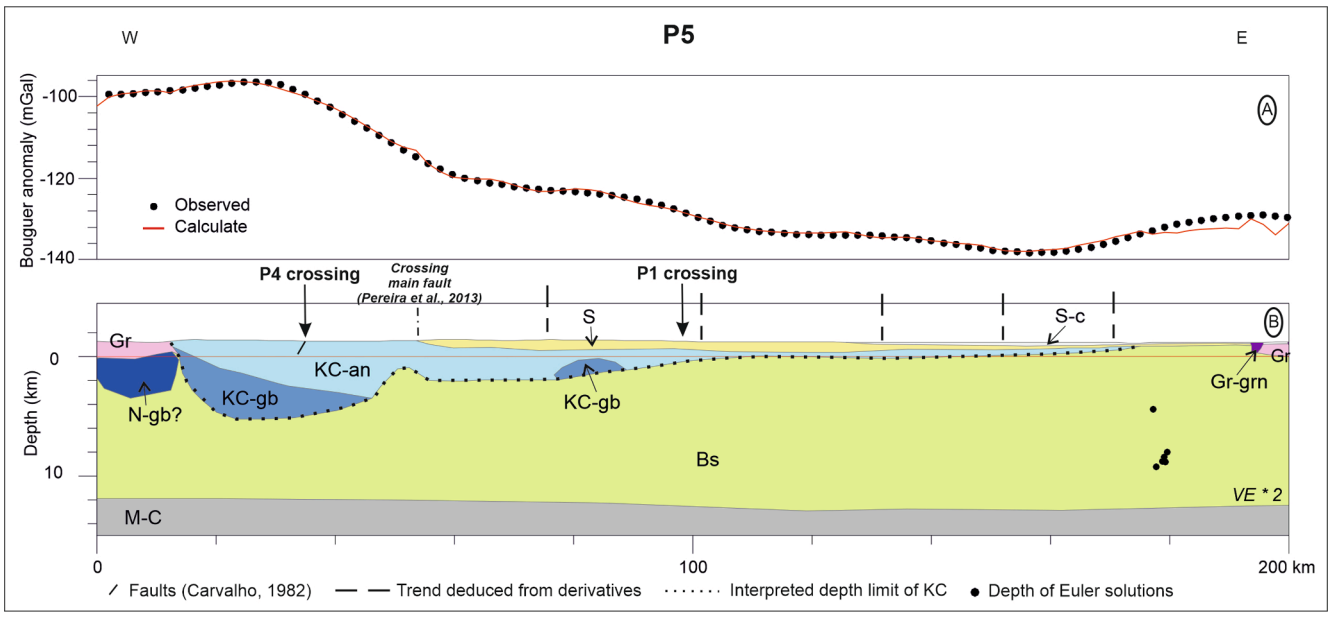

Fig. 8. Bouguer anomaly fitting by the model of the Profile 5 (see Figs. 2 and 3A for location), of 200 km long, is characterized by bodies which configuration is interpreted as: Middle Crust (M–C) and Metasedimentary and igneous derived, as Basement (Bs), Neoarchaean, intruded during eburnean by noritic gabbros (N-gb) and Regional granite (Gr) in the west and Regional Granite to the east, during Palaeoproterozoic. During Mesoproterozoic emplaced the KC (anorthosite, KC-an, and gabbro, KC-gb) crosscutting the basement. In Neogene times the Kalahari units (S and S-c) sedimented from kilometre 60 to the east. Euler solutions are shown in depth. Pointed line represents the interpreted KC boundary in depth with the eastern limit according with some Euler alignment (see Fig. 3A and Fig. 9). Vertical exaggeration 2.

This profile represents the longest profile modelled, and we use it as a test to delimit where there is density deficit or density excess (Fig. 4B). With the constrain of the data provided by CRUST 1.0 model (Laske et al., 2013) we build a simplified two-layers model with the Basement (2.67 g/cm^3) and the Middle Crust (2.8 g/cm^3), obtaining the calculated anomaly; therefore, the observed anomaly data requests dense bodies at both ends of the profile and sparse materials in the central part. By interpreting the geometry of the KC, with both calculated and observed anomalies, a reasonable fitting is achieved.

The starting point while modelling P1 is to set the Middle Crust-Basement boundary, which is located in the SW at 11 km and deepens to the NE up to 13 km.

At the south-westernmost end of the profile, to 40 km, the Bouguer anomaly (Fig. 4C) ranges in an amplitude of up to −80 mGal to −90 mGal, which has been interpreted as related to igneous layering of distinct anorthosite types (white and black anorthosites; Drüppel et al., 2007) of the Zebra Mountains. The Zebra Mountain lobe forms a dome-like anticlinal structure, dipping to the south at relatively steep angles (40°-60°) and to the north at shallower angles (10°-40°) (Maier et al., 2013). The vertical layers of gabbro (KC-gb), with density of 2.81 g/cm^3, provide the maxima value of the Bouguer anomaly data in this part of the profile, while anorthosite layers, with a density of 2.75 g/cm^3 (KC-an, reaching 7 km depth) correspond to the relative gravity minimum (-88 mGal). Although the Euler solutions are scarce here, they perfectly match with the bottom of the anorthosite and gabbroic members of the KC.

From kilometre 40 north-eastward, the Bouguer anomaly increases up to −85 mGal, linked to an extensive mass of gabbros interpreted in the subsurface by high density values (KC-gb, 2.81 g/cm^3) of 5 km depth. At this point, we tested with some different densities and only a body of ~ 2.81 g/cm^3 would fit the anomaly, assigning to the gabbroic unit of KC. The northeaster limit of this gabbroic body is also constrained by some Euler solutions between 6 and 15 km deep. Kilometre 70 sets the outcropping late-Mesoproterozoic olivine-bearing dolerite intrusions (d), (2.70 g/cm^3), found as a thin subhorizontal layer (ca. 500 m thickness) emplaced within the underlying Chela Group (2.68 g/cm^3) and over the KC (Carvalho, 1982; Pereira et al., 2013b).

The Bouguer anomaly slightly decreases between kms 80 and 240, suggesting a large thin anorthosite body (KC-an) that fits this anomaly (delimited by two trends deduced from derivatives), in contrast to both ends of the profile, which are occupied by gabbroic units (KC-gb), with a density of 2.81 g/cm^3. The anorthosite body thins out between kilometres 140 and 280, according to the low values of the Bouguer anomaly. At km 240, the lowest value of ~ 10 mGal coincides with the presence of Upper Kalahari sand deposits (S) that reach up to 500 m of thickness. Haddon (2005), reports 100 m thickness in this area, a divergence that cannot be resolved at the scale of this work. This area also matches with one of the NW-SE main faults defined by Pereira et al. (2013b; see Fig. 2 and Fig. 3A).

From km 270 until the end of the profile, the wide amplitude of the Bouguer anomaly (36 mGal) was interpreted as related to a high-density body (2.81 g/cm^3), which would be associated with subcropping gabbros of the KC. This body is limited southwest and northeast by some Euler solutions ranging from 4 to 15 km. The configuration that best fits the modelling infers a mafic body reaching a depth of 5 km below sea level. These Upper Crustal solutions, placed at the boundaries of the gabbroic units, might be potentially related to a magma-feeding location of the Kunene Complex. The northeastern boundary of the KC, which includes mainly gabbroic with scarce anorthosite components, is approximately located at the km 360 of the profile P1.

Finally, a shallow and thin low-density layer has been linked to Mesoproterozoic red granites (gr) (2.65 g/cm^3), that crop out in the field, and are coeval to the KC intrusion. The northeastern limit of the KC is, in fact, represented by these granite magmas and the scarce anorthosite lithologies that surround them (Fig. 3A and Fig. 4C). Further to the NE, Mesoproterozoic rocks of the KC are absent and the outcropping materials mostly comprise undifferentiated Archaean to Palaeoproterozoic gneisses, migmatites and granites of the Basement.

The P1 gravimetric profile reveals that the KC has a lopolith geometry, with an average maximum depth of 7 km and with a noteworthy elongated NE-SW trend. The gabbroic bodies, found at both ends of the profile, represent ~ 50% of the KC in this modelling, whereas the

anorthosite members, more restricted, thins between km 140 and 280, with a maximum vertical thickness of about 500 m.

PROFILE 2

Profile 2 (Fig. 5) runs 215 km length from W (x = 322300; y = 8182650) to E (x = 535000; y = 8181600), at the southern area of the studied zone (Fig. 2). The outcropping materials consist of metasediments from the Chela Group (Ch) at the westernmost part, which, in turn, are overlaid by dolerite sill-shaped subvolcanic materials (d). The shallow metasedimentary layers of the Chela Group, of ca. 300 m thickness, fit the relative minima from kilometre 13 to 20.

The profile begins with an anomaly of −103 mGal descending to −130 mGal at kilometre 30, (Fig. 5A) which has been related to subcropping noritic gabbros (N-gb, d = 2.85 g/cm^3) from the Eburnean Gabbro-Diorite Complex (Fig. 2 and Fig. 5B), reaching depths of 1.8 km below sea level. Despite the absence of any outcrop of noritic gabbros in the surrounding area (the nearest occurrence is set greater than 50 km to the north), we interpret that denser materials should lie underneath (N-gb, d = 2.85 g/cm^3), keeping this assessment as an open issue. The trend of the overall anomaly on this profile is downward to the east, from −130 mGal at the west to −140 mGal at the easternmost part of the profile. The interpretation of this decay is related to the distinct nature of the basement, which would correspond to upper crustal Neoarchaean metasedimentary and igneous-derived rocks (d = 2.67 g/cm^3) and to a middle crust with a density of 2.8 g/cm^3 (Nafe and Drake, 1957; Rudnick and Fountain, 1995). The regional gravity trend is interrupted by the intrusion of gabbro-anorthositic plutonic bodies of the KC at shallow crustal levels (ca. 3 km; Fig. 5).

The KC represents a large intrusion from kilometre 20 to 180 of the profile, of ca. 5 km thick, with a mean density of 2.75 g/cm^3 in the anorthosite member. The two relative maxima observed between kilometres 30–70 and 100–170 are associated with Mesoproterozoic subcropping gabbros that lie at the bottom of the complex reaching thickness of ca. 3 km representing the denser materials within the KC. Within these relative maxima (between kilometres 70 and 100), the Kunene Complex slightly thins to 2.2 km below sea level, coinciding with a trend deduced from derivatives, fitting the relative minima. While the western gabbroic body is well constrained by the outcropping of KC and the crossing with P1 the eastern body fits the relative gravity maximum together with the alignment of Euler solutions (Fig. 3A) that crosscut this profile, with depths between 3 and 9 km. The eastern boundary of the KC is of particular relevance here to truly evaluate the lateral extent of this body.

Between kilometres 60 and 70, outcropping red granites and rhyolites (gr) (d = 2.65 g/cm^3) represent the lighter units of the Kunene Complex.

From km 146 to the east, a thin layer (less than 200 m thickness; Miller, et al., 2010; Haddon, 2005) of Kalahari sands (S), and sands and clays (S-c) covers the magmatic suites of the KC.

The sharp decrease in the Bouguer anomaly (-140 mGal) from km 160 to the end of the profile, corresponds to the disappearance of KC materials and the thickening and deepening of the basement.

The P2 gravimetric profile confirms the lopolithic shape of the KC, with the gabbroic bodies occupying the bottom of the complex. The KC extends ~ 100 km further east than previously known and has a maximum thickness of 5 km, the uppermost levels of which are composed of anorthosite. The prolongation of the Kunene Complex under the Kalahari sediments depicts the original lopolith-shaped body emplaced during the Mesoproterozoic.

PROFILE 3

Profile 3 (Fig. 6) runs along 190 km from west (x = 378950; y = 8349800) to east (x = 569650; y = 8350400). This profile begins passing through the outcropping Eburnean regional granite (Gr) in the western part, which are intruded by the KC anorthosite bodies at km 17. To the east, Mesoproterozoic red granites (gr) and Kalahari sands (S) are dominantly found between kms 100–130. To the end of the profile, Eburnean granites (Gr) together with scarce Palaeoproterozoic granodiorites and quartz-diorites (Gr-grn) crops out at the surface, almost completely covered by the Kalahari sands.

The modelled profile depicts a Bouguer anomaly ranging from −130 mGal at the east to −87 mGal at the centre of the profile (Fig. 6A). Between kms 0 and 17, the outcropping syn- to late-tectonic Palaeoproterozoic granitoids (Gr) (widespread in the northwestern studied area, see Fig. 2 and Fig. 6B) seems to be related to the relative minima in the Bouguer anomaly (−120 mGal), reaching depths of more than 3 km below sea level by means of a body of 2.65 g/cm^3. From kms 13 to 100, two relative gravity maxima are depicted assuming a positive density contrast between the Archaean basement (2.67 g/cm^3) and the intrusion of Kunene Complex. The first maximum positive relative anomaly found between kms 13 and 45 (-103 mGal) could be justified by the presence of anorthosite (KC-an) layers overlying subcropping gabbros (2.81 g/cm^3), which occur up to 1.6 km depth below sea level, being interpreted as responsible for this positive Bouguer anomaly.

The relative minimum at km 60 corresponds to syn- to late-tectonic Eburnean granitoid bodies (Gr), which extend to 600 m below topographic surface means of densities of 2.65 g/cm^3, and represents a relict body surrounded by the Kunene Complex. To the east, between kms 62 and 110, the second maximum (-87 mGal) is associated to high-density lithologies, such are those attributed to gabbros (KC-gb) from the KC. The gabbroic outcrops found at km 130 of the profile supports this assumption. In this case, these gabbroic magmas thicken up to ca. 5.6 km, in good correspondence with the Bouguer anomaly values. This relative maximum is clearly outlined by Euler solutions, see Fig. 2. The Upper Crust Euler solutions gather at both limits of the gabbroic body, between 6 and 15 km. This eastern boundary of the KC has special relevance for interpreting the extent of this Mesoproterozoic body underneath the Kalahari sands.

To the east, the progressive decrease in the anomaly (up to −130 mGal at the end of the profile) would be justified by a slightly thickened basement (2.67 g/cm^3) and the density contrast with the middle crust (2.80 g/cm^3), together with the presence of a thick (5 km) layer of low-density syn- to late-tectonic granitoids (Gr) (2.65 g/cm^3). At km 130, the sands & clays of the Kalahari reworked (2.0 g/cm^3) extend to km 170, from where the Upper Kalahari sands (S) (2.5 g/cm^3) cover the underlying layers, reaching a thickness of about 400 m to the end of the profile.

Hence, the modelled profile P3, that represents the northern limit of the KC, configures two bodies with variable areas of gabbro and anorthosite. The gabbroic members are located between kms 60 and 120, reaching a maximum depth of 5.6 km (below sea level). Being the northernmost end of the lopolith, the structure seems to be closed by one of the NW-SE fractures (Pereira et al., 2013) and an N-S trend deduced from derivatives.

PROFILE 4

Profile 4 runs along 274 km from northwest (x = 357900; y = 8320900) to southeast (x = 551060; y = 81256500). This profile (Fig. 7) starts in Chibia, where the Eburnean regional granite (Gr) crops out (Fig. 2), and continues southeastward through the KC anorthosites and sparce outcrops of red granites (gr). From km 63 to the end of the profile, Kalahari sands and the reworked Kalahari sands & clays cover the Kunene Complex.

The Bouguer anomaly begins with −113 mGal, increasing up to −97 mGal at km 30. This rising trend is related to the outcropping syn- to late-tectonic Palaeoproterozoic granitoids (Gr), in turn, intruded by interpreted noritic gabbros (N-gb), reaching depths of ~ 1.5 km below sea level.

From kms 22 to 63, anorthosites of the KC crop out, together with scarce coeval red granites and rhyolites (gr). The Kunene Complex extends 5 km below sea level, conforming an elongated lopolith geometry that includes gabbroic lobes at the base. To the northwest, between kms 22 and 52, a gabbroic layer dipping to the southeast justifies the ca. 10 mGal amplitude. To the southeast, between kms 100 and 195, a gabbroic layer gives rise to a relative Bouguer maximum of −110 mGal, being

outlined by Euler solutions (see Fig. 2), with depths between 2.8 and 15 km and NE-SW to N-S trends deduced from derivatives. From km 63 to the end of the profile, the whole KC is covered by Upper Kalahari sands (S) (2.5 g/cm^3), showing a depocenter in km 80, which reaches 3 km in thickness. The last part of the profile is covered by sands & clays of the Kalahari reworked (2.0 g/cm^3).

At the beginning of the profile, the bottom of the basement layer (Bs) is modelled at 11 km depth, gently deepening to 13.5 km at the end of the profile coinciding to a Bouguer relative minimum and the NE-SW fracture (Pereira et al., 2013b), that extends through Caiundo towards eastern Angola (see Fig. 2 and Fig. 3A).

The P4 gravimetric profile endorses the lopolithic shape of the KC. In this case, gabbroic rocks are concentrated in the northwestern edge, conforming a large lenticular body of about 2.5 km thickness, dipping inward the KC. To the SE, gabbroic bodies comprise a structure (~3 km), parallel to the bedding of the enclosing rocks, characterizing the basal section of the complex. The NW-SE trend of P4 provides information of the prolongation of the complex beneath the Kalahari sediments, also revealing the thickening of the Upper Crust (Bs) south-eastward, that coincide with the NE-SW (from Caiundo town to the southwest) main faults that crosses the basement of southern Angola extending more than 400 km (see Fig. 3A).

PROFILE 5

This 200 km long profile runs parallel to and south of Profile 3 (Figs. 2 and 3A), from W (x = 351800; y = 8291800) to E (x = 556700; y = 8291800). It traverses syn- to late-tectonic Eburnean granitoids, anorthosites from the KC, and scarce intrusions of red granites and rhyolites (not represented in the profile), and Kalahari sediments (Fig. 7).

The Bouguer anomaly starts with −100 mGal over the outcrops of Eburnean granitoids (Gr) and associated subcropping noritic gabbros (N-gb), in good agreement with those interpreted in profile 4, with an inferred depth of 4.5 km below the surface. Nevertheless, the existence of some gabbroic bodies from the KC at this location could be a possibility that cannot be ruled out. From km 12 to 54, anorthosites of the KC crop out together with scarce red granites and rhyolites (not shown at the scale of the figure). The decrease of the Bouguer values from −96 mGal at km 22 to −120 mGal at km 60 is related to a thick layer of gabbros underneath (up to 4 km). Toward the east, the Upper Crust (Bs) slightly thickens, reaching a depth of 13 km at km 140 of the profile.

As deduced in the other four modelled profiles, the KC depicts a lopolithic shape, mainly formed by anorthosites and some gabbros at the base. In this case, the KC thins eastwards from 6.5 km thick at km 24 to 300 m thick at km 170. The thinning starts abruptly at km 50 where the decrease in Bouguer anomaly coincides with a crossing main fault (Pereira et al., 2013) and the outcrop of the Kalahari sediments. Within the KC, a ~ 1 km layer of gabbros is located at the centre of the profile between kms 76 and 88.

To the east, the prolongation of the KC beneath the Kalahari sediments is well supported by the N-S alignment of the Euler solutions (Fig. 3A), some of the results shown in this profile, between 4.5 and 9.3 km depth, delimiting the eastward limit of the Complex.

The P5 gravimetric profile helps to define the easternmost limit of the KC (see models shown in Fig. 10). The complex is thicker in the W, reaching a maximum total thickness of 6.5 km, of which 3.8 km is occupied by gabbro (east-dipping), and thins eastwards to a thickness of ~ 300 m (mainly anorthosite lithologies).

6.1. Resume of the modelling

The boundary between Basement and Upper Crust-Middle Crust together with the distinct outcropping units were the main conditioning factors during the modelling process. The two pre-Eburnean basement complexes found at the studied area, the Schist-Quartzite-Amphibolite Complex (SQA) and Jamba Group, and the Gneiss-Migmatite-Granite Complex, are mainly composed of metasedimentary rocks and igneous-derived gneisses that were remobilized during the Eburnean Orogeny (2.0–1.8 Ga). The amphibolite lithologies found within the SQA are interpreted to represent the remnants of a magmatic arc in SW Angola (Rodrigues et al., 2016). For the modelling a standard basement has been used, that might include the two aforementioned bodies, using a density of 2.67 g/cm^3 (Nafe, and Drake, 1957; Rudnick and Fountain, 1995).

Distinct Palaeoproterozoic igneous suites intrude the crystalline basement of the studied area. The Gabbro-Diorite Complex includes granodiorites and quartz-diorites (Gr-grn), dacites, rhyodacites, commonly called quartz-feldspathic porphyries and related rocks, and noritic gabbros (N-gb), with significant calc-alkaline petrochemical features. These rocks are part of a vast Palaeoproterozoic magmatic arc that is well preserved in southwestern Angola (Carvalho, 1982). They represent one of the igneous suites generated during the tectono-thermal Eburnean episode that lasted from about 2.1 Ga until 1.7 Ga (Torquato et al., 1979; Kröner et al., 2010, 2015; De Waele et al., 2008; Rodrigues et al., 2016). These units have been interpreted in profiles 2, 3, 4 and 5, according with the outcrops found in the area, with densities of 2.68 g/cm^3 (Gr-grn) and 2.85 g/cm^3 (N-gb).

The widespread intrusion of Palaeoproterozoic metaluminous to slightly peraluminous granitoids (Regional granite, Gr) in central Angola is well exposed in the modelled profiles (3, 4 and 5). They represent a substantial volume of crust, consisting of arc-derived magmas formed by the recycling and the partial melting of the previously formed crust, that intrude into the gneiss-migmatite basement (Pereira et al., 2003; Carvalho and de Alves, 1993; Jelsma et al., 2011). This gives rise to minimum values of Bouguer Anomaly with density of 2.65 g/cm^3, explained by granite, granodiorite, syenite and rhyolite compositions, conforming irregular shapes from batholith (east of profile 3) to dome (west of profiles 3 and 5), and reaching thickness of more than 4 km.

The late-stages of the Eburnean cycle are associated with the deposition of the volcano-sedimentary units of the Chela Group (Ch and d), that remain undeformed and without metamorphism, presumably formed within a post-orogenic extensional tectonic setting. Density values of 2.68 g/cm^3 for the sedimentary sequences and 2.70 g/cm^3 for the volcanic units and depths below 1000 m were used for this purpose. Maximum depositional U-Pb ages of the Chela Group were determined between 1.79 Ga and 1.75 Ga (Pereira et al., 2011; McCourt et al., 2013), representing the late-stages of the Eburnean orogeny (Epupa Event of Jelsma et al., 2018).

In the Mesoproterozoic, the crystalline basement was intruded by the Kunene Complex (KC) in two phases (Ashwal, 1993). The early phase is dominated by deformed white anorthosite (d = 2.75 g/cm^3) and the late phase corresponds to unaltered anorthosites and gabbroic units (d = 2.81 g/cm^3).

Paleogene-Holocene deposits constitute the younger materials represented in the profiles, with densities of 2.0–2.5 g/cm^3 and maximum depths of 800 m.

7. Discussion

The Kunene Complex of Angola is one of the largest anorthositic massifs on Earth (Ashwal, 1993). The geochemical signatures reported in distinct studies (e.g., Mayer et al, 2004; Baxe, 2007; Drüppel et al., 2007; Brower, 2017) suggest a mantle source for the gabbro-anorthosite members of the Kunene Complex. This mantle source provides such huge amounts of melt that promoted the fractionation and crystallization of vast masses of plagioclase to form large-scale anorthosite massifs (Ashwal, 1993; Drüppel et al., 2007; Gleißner et al., 2011). Multiple authors (e.g., Mayer et al, 2004; Drüppel et al., 2007) ascribed the emplacement of the KC to an intra-continental anorogenic environment, through partial melting of mantle-derived materials that produced the parental magmas of the anorthosites and the scarce mafic related melts, together with anatexis of the lower crust, which promoted the generation of the associated felsic magmas. The similar bimodal magmatic

event recorded at ~ 1375 Ma in the Karagwe–Ankole Belt (KAB) of Central Africa, led Tack et al. (2010) to suggest an intra-cratonic extensional event occurred within the Kibaran belt (the Kibaran Event). Nevertheless, the emplacement of the KC in a contractional regime through progressive ductile thrusting has also been argued, due to the shearing structures found within both the Mesoproterozoic anorthosite and red granite members and their Palaeoproterozoic host-rocks (Lehmann et al., 2020). Due to difficult access and poor exposure, the complex remains relatively poorly studied, especially along its eastern boundary, which is covered by the Kalahari deposits. Combining the available information from the World Gravity Map, petrophysical sampling of some KC units, Euler solutions in depth and 2.5D modelling, some clues are provided to unravel the deep crustal structure of the studied area and to decipher the complete morphology of the anorthositic massif (Fig. 9). To better understand the geometry of the KC and locate its eastern limit under the Kalahari cover, the Fig. 10 shows a 3D view of all analyzed data, i.e. the Euler solutions in depth, the 2.5D profiles and a digitization of the geological units that compose the KC (anorthosites and gabbros).

7.1. Crustal interpretation

The Bouguer anomaly map pictures the transit from oceanic crust to thick lithosphere under the Congo Craton.

The lowest values of Bouguer anomaly are related to the old, light and thick continental crust of the Cassinga Zone (CZ in Fig. 2; Jelsma et al., 2018), representing the Archaean-Palaeoproterozoic crust of the Angolan Central Shield (Congo Craton; Carvalho and de Alves, 1993; Silva, 2005), in which thick lithosphere is found (Pasyanos and Nyblade, 2007). The Congo Craton is understood as an assemblage of distinct Archaean nuclei welded together during the Palaeoproterozoic between 2.1 Ga and 1.8 Ga, related to the amalgamation and formation of the Columbia (Nuna) Supercontinent (Pinna et al., 1996; De Waele et al., 2008; Noce et al., 2007; Delor et al., 2008; Jelsma et al., 2018). In the context of such large-scale thickening, the calculated thickness of this cratonic crust is reasonable.

Following previous works (Torquato, 1977; Coward and Daly, 1984; Pereira et al., 2013b), the area exhibits different structural trends that characterized distinct orogenic cycles. Some pieces of Archaean crust, representing the oldest basement record of the Angola-Kasai Craton, are found at the northeasternmost area of Angola (Northern Lunda region), in Central Angola within the Kwanza Horst and Andulo area, and in southern Angola at the Cassinga Zone. Moreover, Archaean inliers within a dominantly Palaeoproterozoic basement are also a feature of western Angola (Torquato, 1977; Carvalho et al., 2000; Hanson, 2003; Silva, 2005; Pereira et al., 2013b; Jelsma et al., 2018). Nevertheless, the accretionary processes of the Eburnean *s.l.* period significantly modified and remobilized these Archaean structures (e.g., Torquato, 1977; Silva, 2005; Pereira et al., 2013b; Jelsma et al., 2018). The main Palaeoproterozoic directions reported at this SW area of Angola follow two distinct structural trends: i) from the western edge of the KC towards the coastal region the Eburnean *s.l.* macrostructure conforms to a NW-SE-trend; ii) from the NE segment of the KC, NNE-SSW directions dominate the Eburnean trends towards the Huambo area (named as the Quipungo Belt; Torquato et al., 1979). Although the involvement of Mesoproterozoic (Kibaran) compressional processes that affected the crustal structure could not be discarded (Lehmann et al., 2020), the Kunene Complex seems to intrude following the NNE-SSW

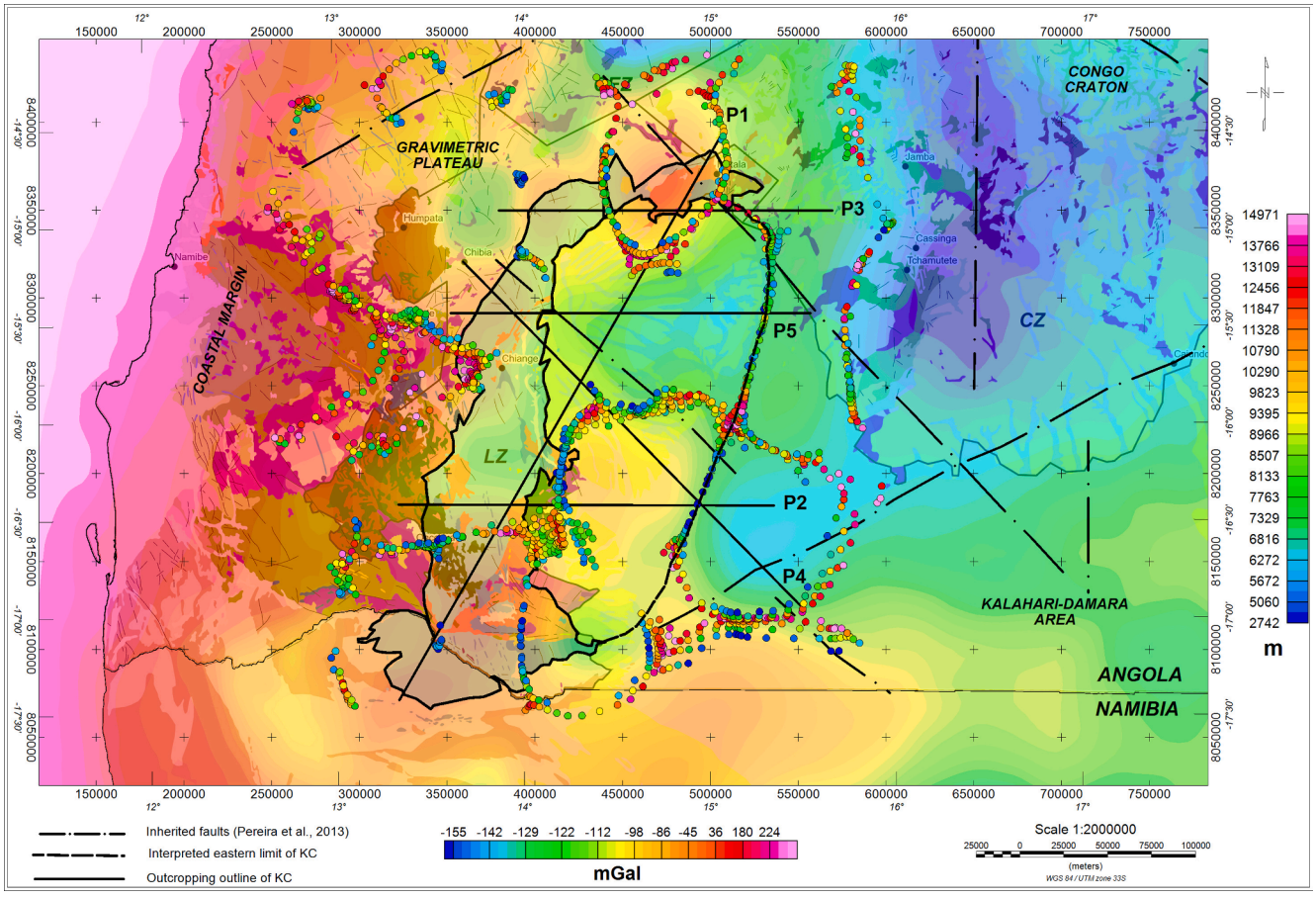

Fig. 9. Geological units (see legend on Fig. 2) and overlying Bouguer anomaly map. Depth Euler solutions are overprinted. The outcrop of the KC is delineated on the west and the deduced extension of the Complex to the east, representing an area at least twice as large (ca. 42500 km^2) as the exposed materials.

Palaeoproterozoic-trend, similar to that found at the southern part of the Moçamedes Arc (Fig. 1). In fact, the boundary between the gravimetric plateau and the Archaean Craton domains (at the Cassinga Zone, CZ in Fig. 2) may be constrained by a N-S to NNE-SSW structure that possibly represents inherited Palaeoproterozoic structures. This structure clearly separates the medium Bouguer anomalies found at the west (gravimetric plateau) and the low values at the east (Cassinga Zone), and probably constitutes a wide zone of lithospheric weakness through which the intrusion of these mantle-derived melts into the crust was harnessed. Such similar crustal scenario leads Tack et al. (2010) to relate the emplacement of the voluminous bimodal magmatism found in the Karagwe-Ankole Belt to an intraplate setting (unsuccessful rift-related intra-plate magmatism), due to the absence of a thick lithospheric profile beneath these mantle-derived magmas, in contrast to their nearby Archaean craton, together with the lack of remnant oceanic crust or juvenile arc-type magmatic rocks in the region. Furthermore, the presence of low-grade Palaeoproterozoic to Mesoproterozoic supracrustal metasedimentary sequences, structured as subhorizontal layers overlying the crystalline basement and the western margin of the KC (Figs. 1, 2, 4 and 5), would suggest an extensional rather than a compressional setting. It is worth to note that Kröner and Rojas-Agramonte (2017) linked some of the metasedimentary sequences found in NW Namibia (the Okapuka Formation), dated at ca. 1320 Ma, to an intracontinental basin, matching them with those metasedimentary rocks exposed at southern Angola (i.e., the Cahama Formation of the Oncocua Region; Carvalho et al., 1987).

On the other hand, the western gravitational limit of the gravimetric plateau with the oceanic crust also follows a NNE-SSW trend, subparallel to the rifted margin (Fig. 3A). This crustal structure would very probably be related to the extensional process related to the Gondwana breakup during the Mesozoic. The inherited structural trends are not apparent towards the coastal margin due to the young thinned crust related to the opening of the South Atlantic oceanic margin. Nevertheless, Torquato (1977) and Carvalho et al. (2000) relate the NNE-SSW structures found at the coastal margin of Angola to the Pan-African orogeny, associated with the Aracuai-Ribeira belt, that connects with the Kaoko belt at the southwesternmost region of Angola, running through the NW of Namibia (e.g., Kröner et al., 2010). These structures have likely localized the continental breakup and *rifting* process during Mesozoic times (Carvalho et al., 2000).

The minimum Bouguer anomaly of the Congo Craton is clearly limited to the south in the Kalahari area by an ENE-WSW-trending structure (running from Caiundo to the SW) that testifies to a large-scale tectonic process.

According to some authors (e.g., Daly, 1988; Hanson, 2003; Goscombe et al., 2017), the Pan-African Damara Belt of Namibia connects with the Lufilian Arc in a NE-SW structural trend beneath the Phanerozoic cover. Some studies suggest that the Angola block behaved as a separated microplate that was accreted to the Congo Craton during the Neoproterozoic (Hanson, 2003; Rapela et al., 2011). The limits of this Angolan microplate are defined by the West-Congo Belt to the north and northeast, the Lufilian Arc to the east and the Damara Belt to the south (Hanson, 2003). However, the scarce geological information and geophysical data of the southern part of Angola has limited the interpretation of the crustal structure below the Kalahari sediments and the connection between the Damara-Lufilian belts. Although the possible linking between these Pan-African belts is beyond the scope of this study, it is apparent that an ENE-WSW-trending structure crosscuts the SE region of the studied area, through Caiundo to the Ruacana region possibly continuing in a WSW to E-W direction in the northwest Namibia, towards the NNW-SSE Kaoko belt.

The possibility that this ENE-WSW-trending structure could be older, affecting the Archaean to Proterozoic crust of southern Angola and northern Namibia, cannot be ruled out. Lehmann et al. (2020) proposed an early phase of ductile deformation before ca. 1680 Ma, that produced WNW-ESE-striking fabrics in the Palaeoproterozoic basement, similar to the metamorphic event proposed by Torquato (1977), named as Namib event (~1675 Ma). The thermal softening associated to the magma ascent in the deep crust during the KC emplacement, from 1500 to 1410 Ma, and the progressive contraction and intrusion of anorthosite sheets resulted in the exhumation and thrusting of the country rocks between 1410 and 1380 Ma with a N-S trend (Lehmann et al., 2020). These structures would have favored the emplacement of the N-S gabbro-norite dykes that crosscut the crystalline basement of SW Angola, including the supracrustal Palaeoproterozoic to Mesoproterozoic metasedimentary sequences, at late-Mesoproterozoic times (i.e., 1.1 Ga; Ernst et al., 2013; Fig. 2 and Fig. 3C).

On the other hand, the geochemical and geochronological studies of the Epupa Metamorphic Complex in northwestern Namibia suggest deformation of the Palaeoproterozoic basement in other distinct episodes. According to Kröner et al. (2010, 2015) the Epupa Complex was first metamorphosed between 1775 and 1750 Ma, whereas later granulite-facies and amphibolite facies metamorphism, occurring between 1450 and 1520 Ma and about 1330 Ma, respectively, were also recorded (Seth et al., 2003; Brandt et al., 2007), conforming with E-W striking shear zones in the Palaeoproterozoic basement. These structures may be correlated, explaining the pronounced E-W elongation and highly altered and deformed KC outcrops in NW Namibia, at the so-called Zebra mountains (Drüppel et al., 2007), and the presence in this area of undeformed nepheline syenite stocks and carbonatite dykes, dated at about 1215 and 1140 Ma (Littmann et al., 2000; Drüppel et al., 2005). Therefore, the ENE-WSW-trending structure found in the southeastern studied region could be related to Mesoproterozoic compressional processes, occurring at about 1330 Ma, and affecting the Archaean to Mesoproterozoic crust of southern Angola and northern Namibia, such as those attributed to the Kibaran Belt (e.g., Cahen et al., 1984). The Kibaran Belt of Central Africa runs from the Democratic Republic of Congo, in a NE-SW direction towards the eastern part of Angola, from where its continuation is uncertain beneath the Kalahari sands (Fig. 1). This interpretation would suggest a possible connection between the Kibaran Belt of eastern Angola towards NW Namibia below the sedimentary cover, forming an arc-shaped structure (NE-SW to ENE-WSW). In addition, it would probably link the KC emplacement with the bimodal extensional magmatism found at this Mesoproterozoic belt in Central Africa, at about 1375 Ma, as suggested by Tack et al. (2010), also arguing for a post-Kibaran compressional event that induced deformation, folding and thrusting of the Archaean, Palaeoproterozoic and early Mesoproterozoic basement. The degree of detail of the source data does not allow us to determine the feeding source, although some hints can be suggested by Euler solutions that show variable deep sources that can be either linked to magma feeding of the KC system, either lithologic change detected in deep which origin is not possible to achieve by this modelling. Since the gabbro-anorthositic members of the Kunene Complex were derived from mantle-derived sources (e.g., Mayer et al., 2004; Drüppel et al., 2007), the geometries determined by the modelling in this work would be compatible with deep mantle-fed channels that progressively gave rise to the voluminous magmatic chamber that conformed the KC.

7.2. KC boundaries

The modelling of five gravimetric profiles serves to delineate the shape of the KC at depth (varying from 1 to 8 km thickness). The modelling leads us to shape a huge anorthositic mass (KC-an), with gabbroic materials at the base (KC-gb), which is surrounded, in its western half, by Palaeoproterozoic granitoid rocks and dense mafic masses (gabbros from the Gabbro-Diorite complex, N-gb), overlaid by low-grade supracrustal rocks, and in the northwest, by the Regional granite (Gr).

The western KC segment is defined by the outcropping lithologies that intrude into the Archaean to Palaeoproterozoic basement in a NNE-SSW trend (Fig. 2) and clearly matches the gravimetric contrasts shown

in the Bouguer anomaly map and the distinct profiles of this study (Figs. 3-8). The intrusion of the KC is synchronous with a progressive contraction, thrusting and exhumation of the basement host-rocks, probably attained during the interval between 1410 and 1380 Ma (Lehmann et al., 2020). Large anorthositic complexes occur in dome-like forms (Buddington, 1939), which appear to have arisen diapirically, displacing high-grade metamorphic rocks (Schrijver, 1975). Nevertheless, an apparent lopolithic morphology is suggested in this modelling, which would be in agreement with the sub-horizontal structure shown by the Palaeoproterozoic to Mesoproterozoic metasedimentary sequences found in the Humpata and the Oncocua regions (Fig. 2).

The Bouguer anomaly map (Fig. 3A) suggests that the intrusion of the KC in the Upper Crust was favored by a large NE-SW to NNE-SSW-trending structure. The connection of the Kibaran Belt from the Democratic Republic of Congo and NE Angola to the southwest (SW Angola and NW Namibia) remains unclear, since this macrostructure was modified during Neoproterozoic times in the region of the Lufilian Arc and its continuation further SW is covered beneath the Kalahari sediments (Fig. 1). Nevertheless, the KC emplacement would be favored by other pre-Mesoproterozoic inherited structures. In fact, it is worth noticing that the shape of the Kunene Complex complies with the NNE-SSW trend that conforms the eastern edge of the Moçamedes Arc (Fig. 1), presumably formed during the Palaeoproterozoic (greater than1675 ± 100 Ma; Torquato, 1977). In any case, it is clear that the KC emplacement took advantage of large-scale weakness structures, noting the opposed trending of basement structures (oriented in ~ NW-SE direction to the west and from N-S to NNE-SSW in the Cassinga Zone) together with the evident contrast of Bouguer anomalies found on both sides of the KC.

The nature and magnitude of plate displacements from Palaeoproterozoic to Neoproterozoic are still controversial, such as between the Congo and Kalahari Cratons (Hanson, 2003) in southern Africa.

Furthermore, this work delimits the easternmost limit of the KC under the tertiary cover, depicted in profiles 2, 3, 4 and 5, when the anomaly curve starts to decline. Further east the anomaly curve falls in concordance with the interpreted thickened crust. Additionally, there is a representative concentration of Euler dataset in this area, and has been additionally used to define the tentative eastern boundary of the KC. The profiles 2, 3 and 4 confirm the eastern limit of KC by the outcropping of the gabbros (profile 3) and the double-crossing within profiles 2 and 4. The N-gb (?) Complex is interpreted as nearby outcrops in the western P5, nevertheless dense masses related to ultramafic/mafic KC could be linked.

The area marked with a dashed-dotted line (Fig. 9), framing the KC to the east, which had not previously been characterized, extends over a hundred kilometers further east than the exposed KC. This implies an area extent of the KC of c. 42500 km^2, calculated from the western outcrops to the eastern extent interpreted at depth from modelling, which means 2.3 times larger than the exposed surface materials (ca. 18000 km^2). The shape of the KC at depth, where no profiles have been done, is highly speculative. Nonetheless, even using a rough calculation of a medium thickness of the KC (~3 km from the five modelled profiles), the resulting volume would be about 112500 km^3.

We propose that the eastern limit of the KC extends more than 100 km further east under the tertiary sediments, making the KC the largest anorthositic intrusion in the world. Nevertheless, more studies (e.g., geochronological, geophysical) are needed to unravel the geological story of this part of Angola.

The resulting models derived in this work may only partially represent the real configuration of the KC due to the non-uniqueness of the gravity method; therefore, some other possible solutions may arise. We use the density as the unique constraint for building the models and delineating the shape of the body. Nevertheless, the knowledge of the geology and the dynamics of the emplacement of anorthosite (e.g. Ashwal, 1993) limit the different options for the regional structure. Although some variations on depth, thickness and shape of the KC are possible, we consider that at such a regional scale the obtained configuration is the most plausible since density contrast and geological geometries fit in a compressible model where unit thickness are preserved and mapping features integrated. Light differences between red granites (2.65 g/cm^3) and basement (2.67 g/cm^3) are appreciable and modelable by fitting gravimetric anomalies. It is worth to emphasize that a net limit between both units represent an analogue of reality, since a nuanced transition would be expected between them. Nevertheless, some isolation is required for modelling and these values have served to carry out the modeling.

7.3. Comparison with large anorthositic complexes and outstanding economic potential of the KC

Massif-type anorthosite complexes were emplaced during a relatively short time interval in the Mid-Proterozoic, particularly in a belt that extends from western USA, through Canada and into Scandinavia (Ashwal, 1993, 2010; Arndt, 2013). The most outstanding outcrops are located in the east of North America, in southern Norway, across Angola and Namibia, at the Kola Peninsula and in eastern Siberia, occasionally accompanied by mineral metallic occurrences. Among them, the largest exposures correspond to the Lac Saint-Jean Complex in Quebec (~17000 km^2), with related Fe-Ti oxide mineralization (Ashwal, 1982), the Kunene Complex (~18000 km^2), containing remarkable reserves of Ti, V, P and REE (Villanova-de-Benavent, et al., 2017), and the Harp Lake Complex in Labrador (~10000 km^2), with associated Ni sulphide ores (Ashwal, 1993), although other minor Mesoproterozoic anorthosite outcrops occur worldwide (see review of Ashwal, 1993). Most of these anorthosite massifs were emplaced between ca. 1.5 and 1.35 Ga, similar to the KC (mainly between 1438 and 1370 Ma, showing felsic-related intrusions from 1503 to 1342 Ma; Mayer et al., 2004; Drüppel et al., 2007; McCourt et al., 2013; Kröner et al., 2015, 2017; Bybee et al., 2019), although Palaeoproterozoic to late-Mesoproterozoic ages were also reported (Ashwal, 1993). When these lithologies are well exposed, the lithological boundaries between the anorthosite bodies and their host-rocks can be determined, as well as the boundaries between individual intrusions that comprise the anorthositic massif (Ashwal, 1993). In fact, at the western segment of the exposed KC, many authors describe magmatic layering and lamination composed of different anorthosite members, probably emplaced over a large time spam (ca. 150–100 Ma), that matches the regional structure of the older basement at the KC margins.

The large new area calculated for the KC via the detailed gravimetric modelling herein, raises the possibility that the KC could increase its economic potential as a source for mineral ores. Recent geochemical studies indicate an enrichment of MgO, Cr, and Ni in distinct lithologies from the Kunene Complex in NW Namibia (Maier et al., 2013), concluding that the potential to host Ni-Cu-rich sulfides is high. In fact, in 2001 the Anglo American company carried out exploration for Ni-Cu sulphide deposits and Ni-Cu-PGE (Platinum Group Elements) in distinct rocks of the KC in the Zebra mountains of Namibia (Haldar, 2017). These Ni–Cu–PGE sulphide mineralisation's occur in small satellite intrusions forming minor deposits in the SW margin of the KC (called as the Ohamaremba troctolite, the Oncocua pyroxenite, and the Ombuku peridotite–gabbronorite; Haldar, 2017).

Recognised potential for economic resources of magnetite, ilmenite and hematite-ilmenite (Ti-Fe) are also reported in the KC (Milesi et al., 2006), together with Ti, V, and possibly P and REE (Villanova-de-Benavent et al., 2017). Magnetite, ilmenite and chromite were reported as cumulus and intercumulus common mineral phases in distinct KC lithologies (e.g., Santos, 1969; Silva, 1992). According to Pereira et al. (2013, and references therein), some titano-magnetite mineralization sparsely occurs associated with gabbroic units and the zoning of light and dark anorthosites, and may accumulate in alluvial deposits. The larger mineralized masses are concentrated in a band extending from Chiange for more than 30 km towards SSW. Santos (1969) estimated at

least 3x10^6 tons of ilmenite in the Chibia region, where outcropping gabbroic rocks are scarcely found (Fig. 2). The presence of a more abundant mafic magmatism at depth, such as the one modeled in this work, would possibly enhance the economic valuation of the KC related to deeper titano-ilmenite mineralized areas.

In Central Africa, Pohl et al. (2013, and references therein) defined the Kibara Metallogenic Province, a huge mineralized region related to the Kibara Belt. This metallogenic domain is composed of two distinct units, that comprise a Ni (Cu, Co, PGE) province of Mesoproterozoic age (ca. 1.4 Ga), associated to mafic–ultramafic intrusions, and a nearly Neoproterozoic (ca. 1 Ga) rare metal (Sn, W, Ta) and Au province, this latter related to the intrusion of late-stage granite-pegmatite melts and associated hydrothermal processes. A considerable potential for Sn–Ta–Be–Li granites, pegmatites and hydrothermal veins, is also reported in this region (Pohl et al., 2013). Although a direct correlation between this mineralized belt and the KC is not completely addressed and the modelling performed in this work does not reveal important Mesoproterozoic granite bodies at depth, the possibility for finding distinct rare and precious metals mineralization's at depth should not be disregarded. Because of the large Kalahari cover, the contribution of geological mapping and exploration in this area is limited. Further drilling and sampling studies would be necessary to suggest the distribution of the mineralization and estimate resources and reserves related to the KC at depth. According to new extent obtained by gravimetric modelling presented in this works, and the eastern boundary of KC underlying the Kalahari sediments, it is suggested that the originally exposed portion of the KC (18000 km^2) is modified by 42500 km^2, what increases its economic potential.

8. Conclusions

We have carried out a gravity study of one of the most remarkable anorthositic complexes in the world: The Kunene Complex. The Bouguer anomaly map pictures the transit from oceanic crust to thick lithosphere under the Congo Craton. The complex lies at the intermediate gravimetric plateau, which is located in a transitional area, between the coastal margin and the Congo Craton-Kalahari Areas. While the western limit is clearly defined, according to the outcropping anorthositic lithologies that intrude into the Archaean to Palaeoproterozoic basement in a NNE-SSW trend, the eastern limit is unexposed under the Kalahari sediments and hence, was unknown until now.

The modelling of five gravimetric profiles helped to unravel the morphology of the crustal materials causing the anomalies, including the eastern limit of the KC. To the west, Eburnean intrusions of gabbros (density 2.81 g/cm^3) and granodiorites/quartz-diorites (density 2.68 g/cm^3) intrude into the metasedimentary and igneous derived basement (density 2.67 g/cm^3). Some of these intrusions reach up to 3 km thick. To the northwest, syn- to late-tectonic Palaeoproterozoic granitoids (density 2.65 g/cm^3) extend as deeper 4 km, and depict a domic morphology. The northeastern limit, although partially hidden by Pleistocene-Paleogene sediments, reveals subcropping denser materials attributed to the metasomatized gabbros from KC, extending to 4 km depth. The KC, formed by anorthosite (density 2.75 g/cm^3) and a large mass of gabbros (density 2.81 g/cm^3), intruded in Mesoproterozoic, forming in a lopolithic shape reaching a preserve thickness of 7 km. The gabbros are more distinct in the western limit and northeastern-southwestern area (Zebra Mountains).

To decipher the eastern prolongation of KC and support the 2.5D modelling, Euler deconvolution have been performed. The N-S alignment of Euler solutions, are in good correspondence with the presence of KC lithologies, is depicted in profiles 2, 3, 4 and 5, and constitutes the data source to derive the eastern KC boundary under the tertiary sediments.

The intrusion of the KC in the Upper Crust was favoured by a large NE-SW to NNE-SSW-trending structure, probably taking advantage of other pre-Mesoproterozoic inherited structures, such as those associated to the Moçamedes Arc. Its emplacement is tentatively linked to the Kibaran extensional event, similar to that described in the Democratic Republic of Congo, according to its lopolithic morphology and the structure of the supracrustal Palaeoproterozoic to Mesoproterozoic metasedimentary sequences. Nevertheless, the possibility of being influenced by late-tectonic Mesoproterozoic orogenic processes cannot be ruled out, taking into account the ENE-WSW-trending structure that is found at the eastern side of the complex that would be probably related to the deformation of the southernmost part of the KC and its Palaeoproterozoic basement (Epupa Complex).

This study helped us to determine the likely volume of this important complex at depth. Although large anorthosites bodies are cataloged in the literature (Ashwal, 2010 and references therein), they are usually associated to other mafic and/or felsic units. In the case of KC, anorthosites make up a dominant part of the intrusive body, being the gabbroic members also outstanding, and hence its high geological interest and its potential as ore source is enhanced from the results of this work. Lateral continuation of KC under the Kalahari sediments is evidenced here, confirming an area at least twice as large (ca. 42500 km^2) as the exposed materials. Hence, this work reveals the likely real dimensions of the anorthositic complex and would open the field for further studies to assess the actual potential and source for mineral ores of the unexposed KC.

CRediT authorship contribution statement

Carmen Rey-Moral: Conceptualization, Methodology, Data curation, Writing – original draft, Writing – review & editing. **Tania Mochales:** Conceptualization, Methodology, Writing – original draft, Writing – review & editing. **Enrique Merino Martínez:** Conceptualization, Writing – original draft, Writing – review & editing. **Jose Luis García Lobón:** Conceptualization. **María Teresa López Bahut:** Data curation. **Raquel Martín-Banda:** Visualization. **María Carmen Feria:** Visualization. **Dianne Ballesteros:** Methodology. **Ana Machadinho:** Visualization. **Daniela Alves:** Visualization.

Declaration of Competing Interest

The authors declare that they have no known competing financial interests or personal relationships that could have appeared to influence the work reported in this paper.

Acknowledgements

Thanks to the Bureau Gravimétrique International, which provided gravity data. We would like to especially thank Isabel Fanlo and Ignacio Subías, who selflessly gave us the samples from the Kunene Complex here shown (University of Zaragoza). Measurements of density were performed in the ISO laboratory of IGME in Tres Cantos (Madrid, Spain). We kindly thank to PLANAGEO project (Plan de Cartografía Geológica, Geofísica y Geoquímica de Angola, IGME-LNEG-IMPULSO Consortium) who provided the anorthosite density data. Dr. Joao Carvalho (LNEG) contributed to improve the manuscript. A. Machadinho acknowledges the support by Geosciences Center of the University of Coimbra (UIDB/00073/2020, FCT). We thank to Dr. Begg and two more reviewers for substantially improve our manuscript.

Appendix A. Supplementary material

Supplementary data to this article can be found online at https://doi.org/10.1016/j.precamres.2022.106790.

References

Alkmim, F.F., Martins-Neto, M.A., 2012. Proterozoic first-order sedimentary sequences of the São Francisco craton, eastern Brazil. Mar. Pet. Geol. 33, 127–139. https://doi.org/10.1016/j.marpetgeo.2011.08.011.

Amante, C., Eakins, B.W., 2009. ETOPO1 1 Arc-Minute Global Relief Model: Procedures, Data Sources and Analysis. NOAA Technical Memorandum. NESDISNGDC-24.

Andrade, M.M., 1962. Sobre a ocorrência de doleritos com augite, enstatite e micropegmatite no Sudoeste de Angola. Estudos Cientificos ofrecidos em homenagem ao Prof. Doutor J. Carrington da Costa. Memória de Junta de Investigacao do Ultramar, Lisboa, pp. 306-495.

Araújo, A.G., Perevalov, O.V., Jukov, R.A., 1988. Carta Geológica de Angola, Escala: 1: 000 000. Instituto Nacional de Geologia, Angola.

Arndt, N., 2013. The formation of massif anorthosite: Petrology in reverse. Geosci. Front. 4 (2), 195–198.

Ashwal, 2010. The temporality of anorthosites. Can. Mineralogist 48, 711–728. https://doi.org/10.3749/canmin.48.4.711.

Ashwal, L.D., 1993. Anorthosites. In: Minerals and Rocks, vol. 21. Springer-Verlag, New York, p. 422 pp..

Ashwal, L.D., 1982. Mineralogy of mafic and Fe-Ti oxide-rich differentiates of the Marcy anorthosite massif, Adirondacks, New York. Am. Mineral 67, 14–27.

Ashwal, L.D., Twist, D., 1994. The Kunene complex, Angola/Namibia: a composite massif-type anorthosite complex. Geol. Mag. 131 (5), 579–591.

Barton, P.J., 1986. The relationship between seismic velocity and density in the continental crust – a useful constraint? Geophys. Jo. R. Astron. Soc. 87 (1), 195–208.

Bassot, J.P., Pascal, M., Vialette, Y., 1981. Données nouvelles sur la stratigraphie, la géochimie et la géochronologie des formations précambriennes de la partie méridionale du Haut Plateau angolais. Bulletin du Bureau de Recherches Géologiques et Mini ères, Section 4. Géologie Générale 4, 285–309.

Baxe, O., 2007. Geocronologia de complexos máfico-ultramáficos: exemplo da série superior do complexo de Niquelândia, Brasil, e do complexo Kunene, Angola. Unpublished PhD Thesis, Universidade de Brasília, Instituto de Geociências, Brazil. 77 pp.

Begg, G.C., Griffin, W.L., Natapov, L.M., O'Reilly, S.Y., Grand, S.P., O'Neill, C.J., Hronsky, J.M.A., Poudjom Djomani, Y., Swain, C.J., Deen, T., Bowden, P., 2009. The lithospheric architecture of Africa: Seismic tomography, mantle petrology, and tectonic evolution. Geosphere 2009 (5), 23–50. https://doi.org/10.1130/GES00179.1.

Blanchar, J., Ernst, R.E., Samson, C., 2017. Gravity and magnetic modelling of layered mafic-ultramafic intrusions in large igneous province plume centre regions; Case studies from the: 1.27 Ga Mackenzie, 1.38 Ga Kunene-Kibaran, 0.06 Ga Deccan and 0.13-0.08 Ga High Arctic events. Can. J. Earth Sci. 54 (3), 290–310. https://doi.org/10.1139/cjes-2016-0132.

Bleeker, W., 2003. The late Archean record: a puzzle in ca. 35 pieces. Lithos 71 (2-4), 99–134.

Bonvalot, S., Balmino, G., Briais, A., Kuhn, M., Peyrefitte, A., Vales N., Biancale, R., Gabalda, G., Moreaux, G., Reinquin, F., Sarrahilh, M., CGMW, 2012. World Gravity Map 1:50M. Bureau Gravimetrique International (BGI). CGMW-BGI-CNES-IRD Ed., Paris. BGI, http://bgi.omp.obs-mip.fr/data-products/Gravity-Databases/Land-Gravity-data.

Braitenberg, C., 2015. Exploration of tectonic structures with GOCE in Africa and across-continents. Int. J. Appl. Earth Obs. Geoinf. 35, 88–95. https://doi.org/10.1016/j.jag.2014.01.013.

Brandt, S., Will, T.M., Klemd, R., 2007. Ultrahigh-temperature metamorphism and anticlockwise PT paths of sapphirine-bearing orthopyroxene-sillimanite gneisses from the Proterozoic Epupa Complex, NW Namibia. Precambr. Res. 153, 143–178.

Brognon, G., 1965. Tectonique et sédimentation dans le Bassin du Cuanza (Angola). Serviços de Geologia e Minas, Angola, T.11, 88 pp.

Brower, A.M., 2017. Understanding Magmatic Timescales and Magma Dynamics in Proterozoic Anorthosites: a Geochronological and Remote Sensing Investigation of the Kunene Complex (Angola). Unpublished PhD Dissertation, University of Witwatersrand, Johannesubrg, South Africa, 86 pp.

Buddington, A.F., 1939. Adirondack igneous rocks and their metamorphism. Geol. Soc. Am. Mem. 7, 1–354.

Bybee, G.M., Hayes, B., Owen-Smith, T.M., Lehmann, J., Ashwal, L.D., Brower, A.M., Hill, C.M., Corfu, F., Manga, M., 2019. Proterozoic massif-type anorthosites as the archetypes of long-lived (≥100 Myr) magmatic systems—New evidence from the Kunene Anorthosite Complex (Angola). Precambr. Res. 332 https://doi.org/10.1016/j.precamres.2019.105393.

Cahen, L., Snelling, N.J., Delhal, J., Vail, J.R., 1984. The Geochronology and Evolution of Africa. Claredon Press, Oxford, p. 512.

Carvalho, H., 1969. Cronologia das formações geológicas Precâmbricas da região central do Sudoeste de Angola e tentaiva de correlação com as do Sudoeste Africano. Bol. Serv. Geol. Minas Angola 20, 61–71.

Carvalho, H., (Coordenador), 1982. Carta Geológica de Angola à escala 1: 1.000.000. Pub. Inst. Inv. Cient. Tropical, Lisboa.

Carvalho, H., 1981. Breves considerações de natureza geológica e de cronologia absoluta sobre as rochas do soco antigo (Arcaico) de Angola. Bol. Soc. Geol. Portugal 22, 307–314.

Carvalho, H., 1972. Chronologie des formations géologiques précambriennes de la région central de South-Ouest de ÍAngola et éssai de corrélation avec celles du Sud-Ouest Africain, 24th Int. Geol. Cong. Montreal, Sect. 1, 187–194.

Carvalho, H., Crasto, J.P., Silva, Z.C.G., Vialette, Y., 1987. The Kibaran Cycle in Angola – a discussion. Geol. J. 22, 85–102.

Carvalho, H., Tassinari, C., Alves, P.H., Guimarães, F., Simoes, M.C., 2000. Geochronological review of the Precambrian in western Angola: links with Brazil. J. Afr. Earth Sc. 31 (2), 383–402.

Carvalho, H., de Alves, P., 1993. The Precambrian of SW Angola and NW Namibia. Com. Inst. Inv. Cient. Tropical, Lisboa, Série Ciências da Terra n° 4, 2–38.

Carvalho, H., de Alves, P., 1990. Gabbro-anorthosite complex of SW Angola/NW Namibia. Instituto de Investigacao Cienifica Tropical, Serie de Ciencias da Terra. In: Com. No., 2. Dept. Ciencias da Terra, Lisboa, p. 66.

Cooper, G.R.J., Cowan, D.R., 2011. A generalized derivative operator for potential field data. Geophys. Prospect. 59, 188–194. https://doi.org/10.1111/j.1365-2478.2010.00901.x.

Coward, M.P.C., Daly, M.C., 1984. Crustal lineaments and shears zones in Africa: their relationships to plate movements. Precambr. Res. 24, 27–45.

Daly, M.C., 1988. Crustal Shear Zones in Central Africa: a Kinematic Approach to Proterozoic Tectonics. Episodes 11 (1), 5–11.

De Waele, B., Johnson, S.P., Pisarevsky, S.A., 2008. Paleoproterozoic to Neoproterozoic growth and evolution of the eastern Congo Craton: Its role in the Rodinia puzzle. Precambr. Res. 160, 127–141.

De Wit, M.J., Linol, B., 2015. Precambrian Basement of the Congo Basin and its flanking terrains. In: De Wit, M.J. (Ed.), Geology and Resource Potential of the Congo Basin. Springer-Verlag, Berlin Heidelberg, Regional Geology Reviews, p. 417.

Delhal, J., Ledent, D., Pastels, P., 1975. L'age du complexe granitique et migmatitic de Dibaya (region du Kasai, Zaire) par lês méthodes Rb-Sr et U-Pb. Ann. Soe. Géol. Belg. 98, 141–154.

Delor, C., Theveniaut, H., Cage, M., Pato, D., Lafon, J.M., Bialkowski, A., Roig, J.Y., Neto, A., Cavongo, M., Sergeev, S., 2008. New insights into the Precambrian geology of Angola: Basis for an updated lithochronological framework at 1:2000000 scale. 22nd Colloquium of African Geology. 52-53.

Delor, C., Lafon, J.M., Rossi, P., Cage, M., Pato, D., Chevrel, S.L., Metour, J., Matukov, D., Sergeev, S., 2006. Unravelling Precambrian crustal growth of central west Angola: Neoarchaean to Siderian inheritance, main Orosirian accretion and discovery of the "Angolan" Pan African Belt. In: In Abstract of the 21st Colloquium of African Geology, pp. 3–5.

Drüppel, K., Littmann, S., Romer, R.L., Okrusch, M., 2007. Petrology and isotope geochemistry of the Mesoproterozoic anorthosite and related rocks of the Kunene. Intrusive Complex, NW Namibia. Precambr. Res. 156 (1–2), 1–31. https://doi.org/10.1016/j.precamres.2007.02.005.

Drüppel, K., Hoefs, J., Okrusch, M., 2005. Fenitizing processes induced by ferrocarbonatite magmatism at Swartbooisdrif, NW Namibia. J. Petrol. 46, 377–406.

Ernst, R.E., Pereira, E., Hamilton, M.A., Pisarevsky, S.A., Rodrigues, J.F., Tassinari, C.G. C., Teixeira, W., Van-Dunem, V., 2013. Mesoproterozoic intraplate magmatic "barcode" record of the Angola portion of the Congo craton: newly dated magmatic events at 1500 and 1110 Ma and implications for Columbia (Nuna) supercontinent reconstructions. Precambr. Res. 230, 103–118.

Evans, D.A.D., 2013. Reconstructing pre-Pangean supercontinents. Geol. Soc. Am. Bull. 125, 1735–1751.

Finn, C.A., Bedrosian, P.A., Cole, J.C., Khoza, T.D., Webb, S.J., 2015. Mapping the 3D extent of the Northern Lobe of the Bushveld layered mafic intrusion from geophysical data. Precambr. Res. 268, 279–294. https://doi.org/10.1016/j.precamres.2015.07.003.

Fullea, J., Fernàndez, M., Zeyen, H., 2008. FA2BOUG—A FORTRAN 90 code to compute Bouguer gravity anomalies from gridded free-air anomalies: application to the Atlantic-Mediterranean transition zone. Comput. Geosci. 34 (12), 1665–1681.

Gleißner, P., Drüppel, K., Taubald, H., 2011. Magmatic evolution of Anorthosites of the Kunene Intrusive Complex, NW Namibia: evidence from oxygen isotope data and trace element zoning. J. Petrol. 51 (4), 897–919. https://doi.org/10.1093/petrology/egq005.

Goscombe, B., Foster, D.A., Gray, D., Wade, B., Marsellos, A., Titus, J., 2017. Deformation correlations, stress field switches and evolution of an orogenic intersection: The Pan-African Kaoko-Damara orogenic junction, Namibia. Geosci. Front. 8 (6), 1187–1232.

Haddon, I.G., 2005. The Sub-Kalahari geology and tectonic evolution of the Kalahari basin, Southern Africa. University of the Witwatersrand, Johannesburg, South Africa, p. 343 pp.. Ph.D. Thesis.

Haldar, S.K., 2017. Chapter 3. Deposits of Africa. In: Haldar, S.K. (Ed.), Platinum-Nickel-Chromium Deposits. Geology, Exploration and Reserve Base, Ed. Elsevier. https://doi.org/10.1016/C2014-0-00851-9.

Hanson, R.E., 2003. Proterozoic geochronology and tectonic evolution of southern Africa. Geol. Soc., London, Special Publications 206 (1), 427–463.

Jelsma, H.A., McCourt, S., Perritt, S.H., Armstrong, R.A., 2018. The Geology and Evolution of the Angolan Shield, Congo Craton. In: Siegesmund, S., Basei, M., Oyhantçabal, P., Oriolo, S. (Eds.), Geology of Southwest Gondwana, Regional Geology Reviews. Springer, Cham. https://doi.org/10.1007/978-3-319-68920-3_9.

Jelsma, H., Perritt, S.H., Armstrong, R.A, Ferreira, H.F., 2011. SHRIMP U-Pb zircon geochronology of basement rocks of the Angolan Shield, western Angolan. In: Proceedings of the 23rd CAG, Johannesburg, Council for Geoscience, Pretoria, 203.
Johnson, G.R., Olhoeft, G.R., 1984. Density of rocks and minerals: in Carmichael. R. S., Ed., Handbook of physical properties of rocks. CRC Press 3, 1–38.
Kampunzu, A.B., Rumvegeri, B.T., Kapenda, D., Lubala, R.T., Caron, J.P., 1986. Les Kibarides d'Afrique centrale et orientale: une belte de collision. UNESCO, Geol. Econ. Dev., Newslett. 5, 125–137.
Keating, P.B., 1998. Weighted Euler deconvolution of gravity data. Geophysics 63, 1595–1603. https://doi.org/10.1190/1.1444456.
Kokonyangi, J., Kampunzu, A.B., Poujol, M., Okudaira, T., Yoshida, M., Shabeer, K.P., 2005. Petrology and Geochronology of Mesoproterozoic mafic-intermediate plutonic rocks from Mitwaba (D.R. Congo): implications for the evolution of the Kibaran belt in central Africa. Geol. Mag. 142 (I), 109–130.
Kopershoek, H.R., 1970. Geology of the Cassinga north area; explanatory note of the 1/50,000 geological map. Rel. inéd. Comp. Min. Lobito, Div. Prosp. Cassinga, Jamba.
Kröner, A., Rojas-Agramonte, Y., 2017. Mesoproterozoic (Grenville-age) granitoids and supracrustal rocks in Kaokoland, northwestern Namibia. Precambr. Res. 298, 572–592.
Kröner, A., Rojas-Agramonte, Y., Wong, J., Wilde, S.A., 2015. Zircon reconnaissance dating of proterozoic gneisses along the Kunene River of northwestern Namibia. Tectonophysics 662, 125–139.
Kröner, A., Vermelhas-Agramonte, Y., Hegner, E., Hoffman, K.H., Wingate, M.T.D., 2010. SHRIMP zircon dating and Nd isotopic systematics of Paleoproterozoic migmatitiv orthognaissses in the Epupa Metamorphic Complex of northwest Namíbia. Precambr. Res. 183, 50–69.
Kröner, A., Stern, R.J., 2005. Pan-African Orogeny. In: Selley, R.C., Cocks, L.R.M., Plimer, I.R. (Eds.), Encyclopaedia of Geology, vol. 1. Elsevier, Amsterdam, pp. 1–12.
Kröner, A., Cordani, U., 2003. African, southern Indian and South American cratons were not part of the Rodinia supercontinent: evidence from field relationships and geochronology. Tectonophysics 375 (1-4), 325–352.
Kröner, A., Correia, H., 1980. Continuation of the Pan African Damara Belt into Angola: a proposed correlation of the Chela Group in Southern Angola with the Nosib Group in Northern Namibia/SWA. Trans. geol. Soc. S. Afr. 83, 5–16.
Laske, G., Masters, G., Ma, Z. and Pasyanos, M., Update on CRUST1.0 - A 1-degree Global Model of Earth's Crust, Geophys. Res. Abstracts, 15, Abstract EGU2013-2658, 2013.
Lehmann, J., Bybee, G.M., Hayes, B., Owen-Smith, T.M., Belyanin, G., 2020. Emplacement of the giant Kunene AMCG complex into a contractional ductile shear zone and implications for the Mesoproterozoic tectonic evolution of SW Angola. Int. J. Earth Sci. 109, 1463–1485. https://doi.org/10.1007/s00531-020-01837-5.
Littmann, S., Romer, R.L., Okrusch, M., 2000. Nephelinsyenite der Epembe-Swartbooisdrif-Alkali-Provinz (ESAP)/ NW Namibia. Berichte der deutschen Mineralogischen Gesellschaft. Beihefte zum Eur. J. Miner. 12, 115.
Lowrie, W., 1997. Fundamentals of Geophysics. Cambridge University Press.
Maier, W.D., Rasmussen, B., Fletcher, I.R., Li, C., Barnes, S.-J., Huhma, H., 2013. Society of Economic Geologist, Inc. Econ. Geol. 108, 953–986.
Marsh, J.S., Swart, R., 2018. The Bero Volcanic Complex: extension of the Paraná-Etendeka Igneous Province into SW Angola. J. Volcanol. Geoth. Res. 355, 21–31.
Marzoli, A., Melluso, L., Morra, V., Renne, P.R., Sgrosso, I., D'Antonio, M., Duarte Morais, M., Morais, E.A.A., Ricci, G., 1999. Geochronology and petrology of Cretaceous basaltic magmatism in the Kwanza basin (western Angola), and relationships with the Paraná -Etendeka continental flood basalt province. J. Geodyn. 28, 341–356.
Matmon, A., Hidy, A.J., Vainer, S., Crouvi, O., Fink, D., Erel, Y., Chazan, M., 2015. New chronology for the southern Kalahari Group sediments with implications for sediment-cycle dynamics and early hominin occupation. Quat. Res. 84 (1), 118–132.
Mayer, A., Hofmann, A.W., Sinigoi, S., Morais, E., 2004. Mesoproterozoic Sm–Nd and U-Pb ages for the Kunene Anorthosite Complex of SW Angola. Precambr. Res. 133 (3–4), 187–206. https://doi.org/10.1016/j.precamres.2004.04.003.
McCourt, S., Armstrong, R.A., Jelsma, H., Mapeo, R.B.M., 2013. New U-Pb SHRIMP ages from the Lubango region, SW Angola: Insights into the Palaeoproterozoic evolution of the Angolan Shield, southern Congo Craton, Africa. J. Geol. Soc. 170 (2), 353–363.
Meert, J.G., 2012. What's in a name? The Columbia (Paleopangea/Nuna) Supercontinent. Gondwana Res. 21, 987–993.
Milesi, J.P., Toteu, S.F., Deschamps, Y., Feybesse, J.L., Lerouge, C., Cocherie, A., Penaye, J., Tchameni, R., Moloto-A-Kenguemba, G., Kampunzu, H.A.B., Nicol, N., Duguey, E., Leistel, J.M., Saint-Martin, M., Ralay, F., Heinry, C., Bouchot, V., Doumnang Mbaigane, J.C., Kanda Kula, V., Chene, F., Monthel, J., Boutin, P., Cailteux, J., 2006. An overview of the geology and major ore deposits of Central Africa: explanatory note for the 1:4.000.000 map "Geology and major ore deposits of Central Africa". J. Afr. Earth Sc. 44 (4-5), 571–595.
Miller, R.McG., Pickford, M., Senut, B., 2010. The Geology, Palaeontology and Evolution of The Etosha Pan, Namibia: Implications For Terminal Kalahari Deposition. South African J. Geol. 113 (3), 307–334.
Morais, E., Sinigoi, S., Mayer, A., Mucana, A., Miguel, L.G., Neto, J., 1998. The Kunene Gabbro-anorthosite Complex: preliminary results based on new field and chemical data. Africa Geosci. Rev. 5, 14.
Nafe, J.E., Drake, C.L., 1957. Variation with depth in shallow and deep-water marine sediments of porosity, density and the velocities of compressional and shear waves. Geophysics 22 (3), 523–552.
Nicolai, C.von., Scheck-Wenderoth, M., Warsitzka, M., Schødt, N., Andersen, J., 2013. The deep structure of the South Atlantic Kwanza Basin — Insights from 3D structural and gravimetric modelling. Tectonophysics 604, 139–152. https://doi.org/10.1016/j.tecto.2013.06.016.
Noce, C.M., Pedrosa-Soares, A.C., da Silva, L.C., Armstrong, R., Piuzana, D., 2007. Evolution of polycyclic basement complexes in the Aracuai Orogen, based on U-Pb SHRIMP data: Implications for Brazil-Africa links in Paleoproterozoic time. Precambr. Res. 159, 60–78.
Pasyanos, M.E., Nyblade, A.A., 2007. A top to bottom lithospheric study of Africa and Arabia. Tectonophysics 444, 27–44. https://doi.org/10.1016/j.tecto.2007.07.008.
Pavlis, N.K., Holmes, S.A., Kenyon, S.C., Factor, J.K., 2008. An Earth Gravitational Model to degree 2160: EGM2008. General Assembly of the. European Geosciences Union, Vienna, Austria.
Pereira, E., 1977. Serra da Neve (Angola). Nota sobre a geomorfologia da região e idade das aplanações. Boletim da Sociedade Geológica de Portugal XX, 277–282.
Pereira, E., 1971. Nota sobre o Complexo ígneo ante-Apciano do Cuanza-Sul (Angola). Bul. Serv. Geol. Minas de Angola 23, 51–80.
Pereira, E., Rodrigues, J., Tassinari, C.G., Van-Dúnen, M.V., 2013a. Carta Geológica de Angola escala 1: 250 000: Folha Sul D-33/T (Chibia). Pub. Inst. Geol Angola.
Pereira, E., Rodrigues, J., Tassinari, C.G., Van-Dúnen, M.V., 2013b. Geologia da região de Lubango, SW de Angola Evolução no contexto do cratão do Congo. Pub. Inst. Geol. Angola, 141 pp.
Pereira, E., Tassinari, C.G., Rodrigues, J.F., Van-Dúnen, M.V., 2011. New data on the deposition age of the volcano-sedimentary Chela Group and its Eburnean basement: implications to post-Eburnean crustal evolution of the SW of Angola. Comunicacoes Geológicas do LNEG 98, 29–40.
Pereira, E., Rodrigues, J., Reis, B., 2003. Synopsis of Lunda geology, NE Angola: Implications for diamond exploration. Comun. Inst. Geol. e Mineiro, t. 90, 189–212.
Pérez-Díaz, L., Eagles, G., 2014. Constraining South Atlantic growth with seafloor spreading data. Tectonics 33 (9), 1848–1873. https://doi.org/10.1002/2014TC003644.
Pinna, P., Cocherie, A., Thiéblemont, D., Feybesse, J.-L., Lagny, P., 1996. Evolution géodynamique du Craton Est-Africain et déterminisme lîtologique. Geodynamic evolution and metallogenic controls in the East-African Craton (Tanzania, Kenya, Uganda). Bureau des Researches Géologiques et Minières, Chroniques des Recherches Minières 525, 33–43.
Pohl, W.L., Biryabarema, M., Lehmann, B., 2013. Early Neoproterozoic rare metal (Sn, Ta, W) and gold metallogeny of the Central Africa Region: a review. Applied Earth 66 Science (Trans. Inst. Min. Metall. B) 122 (2), 66–82.
Rapalini, A.E., 2013. The Assembly of Western Gondwana: Reconstruction Based on Paleomagnetic Data. In: Siegesmund, S. (Ed.), Geology of Southwest Gondwana. Springer International Publishing AG, Regional Geology Reviews, pp. 1–16.
Rapela, C.W., Fanning, C.M., Casquet, C., Pankhurst, R.J., Spalletti, L., Poiré, D., Baldo, E.G., 2011. The Rio de la Plata craton and the adjoining Pan-African/brasiliano terranes: their origins and incorporation into south-west Gondwana. Gondwana Res. 20 (4), 673–690.
Reid, A.B., Ebbing, J., Webb, S.J., 2014. Avoidable Euler Errors - the use and abuse of Euler deconvolution applied to potential fields. Geophys. Prospect. 62, 1162–1168. https://doi.org/10.1111/1365-2478.12119.
Rodrigues, J.F., Pereira, E.S., Tassinari, C.C., Van Dúnem, M.V., 2016. Paleoproterozoic Magmatic Arc in SW of Angola (Congo Craton SW border): petrochemical evidences and geochronological data. In: 35th International Geological Congress Abstracts, Cape Town, South Africa. 5583.
Rudnick, R.L., Fountain, D.M., 1995. Nature and composition of the continental crust: a lower crustal perspective. Rev. Geophys. 33–3, 267–309.
Salminen, J., Hanson, R., Evans, D.A.D., Gong, Z., Larson, T., Walker, O., Gumsley, A., Söderlund, U., Ernst, R., 2018. Direct Mesoproterozoic connection of the Congo and Kalahari cratons in proto-Africa: Strange attractors across supercontinental cycles. Geology 46 (11), 1011–1014.
Santos, L., 1969. Ocorrências de ilmenites no Sul de Angola. Bol. Serviços de Geologia e Minas de Angola 20, 8–21.
Schannor, M., Lana, C., Fonseca, M.A., 2019. São Francisco-Congo Craton break-up delimited by U-Pb–Hf isotopes and trace-elements of zircon from metasediments of the Araçuaí Belt. Geosci. Front. 10 (2), 611–628. https://doi.org/10.1016/j.gsf.2018.02.011.
Schrijver, K., 1975. Deformed rock of a composite diapir in granulite facies. Geotekt. Forsch 49, 1–118.
Seth, B., Armstrong, R.A., Brandt, S., Villa, I.M., Kramers, J.D., 2003. Mesoproterozoic U-Pb and Pb-Pb ages of granulites in NM Namíbia: Reconstructing a complete orogenic cycle. Precambr. Res. 126, 147–168.
Silva, A.T.F., 2005. A geología da República de Angola desde o Paleoarcaico ao Paleozóico Inferior. Instituto Nacional de Engenharia, Tecnologia e Inovação, IP, p. 45.
Silva, Z.C.G., 1992. Mineralogy and cryptic layering of the Kunene anorthosite complex of SW Angola and Namibia. Mineral. Mag. 56 (384), 319–327.

Silva, A.T.F., Torquato, J.R., Kawashita, K., 1973. Alguns dados geocronológicos pelo método K/Ar da região de Vila Paiva Couceiro, Quilengues e Chicomba (Angola). Serviço de Geologia e Minas de Angola, Bol. 24, 29–46.

Silveira, E.M., Söderlund, U., Oliveira, E.P., Ernst, R.E., Menezes, L., 2013. First precise U-Pb Baddeleyite Ages of 1500 Ma Mafic Dykes from the Sao Francisco Craton, Brazil, and Tectonic implications. Lithos 174, 144–156.

Slejko, F.F., Demarchi, G., Morais, E., 2002. Mineral chemistry and Nd isotopic composition of two anorthositic rocks from the Kunene complex (South Western Angola). J. Afr. Earth Sc. 35 (1), 77–88.

Tack, L., Wingate, M.T.D., De Waele, B., Meert, J., Belousova, E., Griffin, B., Tahon, A., Fernandez-Alonso, M., 2010. The 1375 Ma Kibaran event in Central Africa: prominent emplacement of bimodal magmatism under extensional regime. Precambr. Res. 180, 63–84. https://doi.org/10.1016/j.precamres.2010.02.022.

Telford, W.M., Geldart, L.P., Sheriff, R.E., Keys, D.A., 1976. Applied Geophysics. Cambridge University Press, Cambridge, p. 860.

Thompson, D.T., 1982. EULDPH: A new technique for making computer-assisted depth estimates from magnetic data. Geophysics 47, 31–37. https://doi.org/10.1190/1.1441278.

Torquato, J.R., 1977. Geotectonic outline of Angola. Cahiers O.R.S.T.O.M., Sér. Géol., Paris, IX, 15–34.

Torquato, J.R., Salgueiro, M.A.A., 1977. Sobre a idade de algumas rochas da região do Cahama (Folha geológica no 399). Angola. Bol. Inst. Geociências Univ. São Paulo 8, 97–106.

Torquato, J.R., Ferreira da Silva, A.T.S., Cordani, U.G., Kawashita, K., 1979. A evolução geológica do Cinturão Móvel do Quipungo no Ocidente de Angola. An. Acad. Brasil. Ciên. 51 (1), 133–144.

Villanova-de-Benavent, C., Torró, L., Castillo-Oliver, M., Campeny, M., Melgarejo, J.C., Llovet, X., Galí, S., Gonçalves, A.O., 2017. Fe–Ti (–V) Oxide Deposits of the Kunene Anorthosite Complex (SW Angola). Mineral. Thermo-Oxybarometry. Minerals 7 (12), 246. https://doi.org/10.3390/min7120246, 27 pp.